GE PANAMETRICS
Waltham, MA 02453

TITLE

Electron Calibration Report

GOES NO/PQ MAGED Telescope

Engineer	Configuration Control
11/23/04	for D.C. 11/23/04
Product Assurance	Program Physicist
11/22/04	11/23/04
Program Manager	Program Engineer
11/23/04	11/23/04

SIZE	DRAWING NUMBER	REV
A	GOESN-ENG-028	-

SHEET 1 OF 50

RELEASE AND REVISION RECORD

Rev.	Authority	Description	Release	
			Date	Approved
-	F. Hanser	Initial Release	11/23/04	F. G. H.

TABLE OF CONTENTS

LIST OF FIGURES

LIST OF TABLES

1.0 INTRODUCTION

1.1 Purpose

This report presents the results of the particle calibration of the EM MAGED Telescope No. 1 performed using the (high energy) electron beam from the MIT Van de Graaff (VdeG) accelerator in Building N-10 at MIT, Cambridge, MA; the (low energy) electron beam from the Cockroft-Walton accelerator at the GSFC Radiation Effects Laboratory in Greenbelt, MD; and the (high energy) proton VdeG accelerator at the GSFC Radiation Effects Laboratory in Greenbelt, MD. The data have been reduced to the geometric factors necessary to convert the nME1 through nME5 (n = 1 through 9, for the MAGED telescopes) electron channel telemetry data into electron fluxes, and to correct the data for proton flux contamination using the MAGPD proton flux data. Some of the measured area vs. angle data are also given, to provide information on the angular responses of the MAGED electron channels.

1.2 Reference Documents

Table 1-1 lists the documents referenced in this report. The first is the test procedure used to acquire the data, while the second and third are the Calibration Report and Accelerator Calibration Test Procedure for the identical electron telescope design used in the TIROS/NOAA spacecraft SEM-2 MEPED. The last three references are the tabulated stopping powers used for the calculated responses, as well as corrections to the measured beam energies by monitor detectors.

Table 1-1. Referenced Documents

Ref. #	Report Number	Date	Title
1	GOESN-RTP-136, Rev. -	Run Aug. – Sept., 2004	Procedure, Electron Calibration, MAGED
2	TIR-ENG-116, Rev. -	July 27, 1994	TIROS SEM-2 PM MEPED/SN 0010 Calibration Report
3	TIR-RTP-156, Rev. -	May 8, 1991	Test Procedure, MEPED Accelerator Calibration
4	NASA SP-3012	1964	Tables of Energy Losses and Ranges of Electrons and Positrons; M. J. Berger and S. M. Seltzer
5	NASA SP-3036	1966	Additional Stopping Power and Range Tables for Protons, Mesons, and Electrons; M. J. Berger and S. M. Seltzer
6	Atomic Data and Nuclear Data Tables	Vol. 27, Nos. 4/5, July/September 1982	Proton Range-Energy Tables, 1 keV – 10 GeV, Part 2, Elements; J. F. Janni

1.3 Acronym List

The acronyms used in this report are listed in Table 1-2.

Table 1-2. List of Acronyms

Acronym	Definition
1MEi	Electron channel "i" in electron telescope 1 of the MAGED ("i" = 1 to 5)
nMEi	Electron channel "i" in electron telescope n of the MAGED ("i" = 1 to 5)
EM	Engineering Model
EPS	Energetic particle Sensor
FOV	Field-of-View
GOES NOPQ	Geostationary Operational Environmental Satellite N, O, P, and Q
GSFC	Goddard Space Flight Center
IFC	In Flight Calibration
MAGED	Magnetospheric Electron Detector
MAGPD	Magnetospheric Proton Detector
MEPED	Medium Energy Electron and Proton Detector
MIT	Massachusetts Institute of Technology
MF	Major Frame
Mf	Minor Frame
NOAA	National Oceanic and Atmospheric Administration
PM	Protoflight Model
SEM	Space Environment Monitor
SEM-2	Space Environment Monitor 2 (TIROS/NOAA spacecraft)
SSD	Solid State Detector
TIROS	Television Infra-Red Observational Satellite
VdeG	Van de Graaff Accelerator

2.0 GEOMETRIC FACTOR DEFINITION AND MEASUREMENT

2.1 Geometric Factor Definition

The geometric factors of the 1ME1 through 1ME5 electron channels are defined by an integral of the detection area over solid angle. A detection area of $A(E,\Omega)$ cm^2 for electrons of energy E MeV and angle Ω, the geometric factor G(E) is given by

$$G(E) = \int A(E,\Omega)\, d\Omega \ cm^2\text{-sr} \qquad (2.1)$$

where $d\Omega = (\sin\theta)\, d\theta\, d\varphi$, with θ the elevation angle and φ the azimuth angle. For an isotropic electron flux J(E) el/(cm^2-s-sr) the channel count rate is given by

$$C_{el} = \int J(E)\, G(E)\, dE \ s^{-1} \qquad (2.2)$$

For an electron flux where there is also an angle dependence, the channel count rate is given by

$$C_{el} = \int J(E,\Omega)\, A(E,\Omega)\, dE\, d\Omega \ s^{-1} \qquad (2.3)$$

For normal conditions the geometric factor (2.1) is used, with the count rate given by (2.2).

The design of the MAGED telescopes is shown in Figure 2-1, with all nine (9) telescopes being identical. The telescope FOV is cylindrically symmetric, with a full width of 30 degrees.

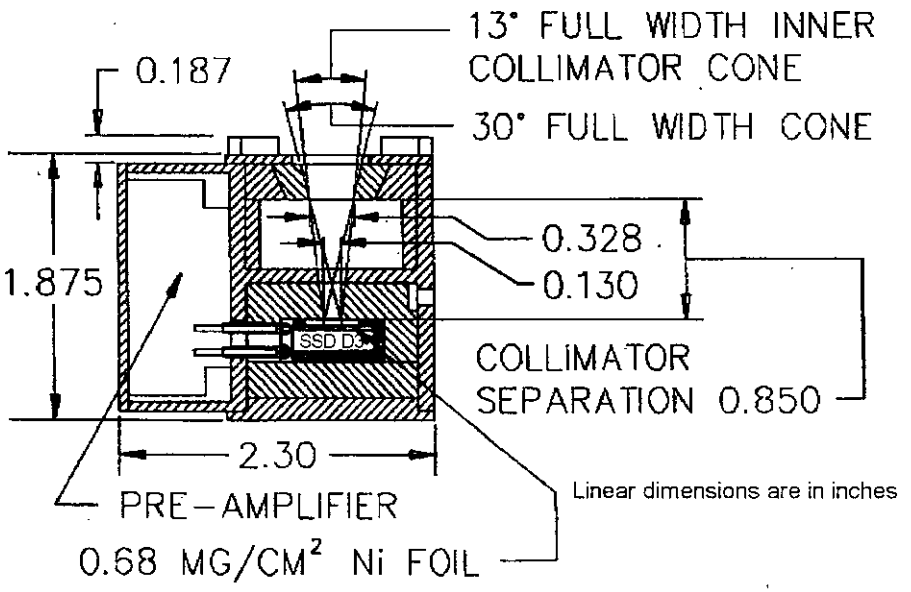

Figure 2-1. MAGED Telescope Design and FOV

2.2 Experimental Measurement of the Geometric Factor

The experimental measurement of G(E) is done by measuring the angular response A(E,Ω) at several angles. The integrated geometric factor is then calculated by a numerical sum

$$G(E) = \sum_i A(E,\Omega_i)\,\Delta\Omega_i \qquad (2.4)$$

where

$$\Delta\Omega_i = 2\pi \times (\cos\theta_{1i} - \cos\theta_{2i}) \qquad (2.5)$$

with θ being the polar angle from the FOV center and 2π being the full rotational angle. Measurements are made at sets of angles θ_i, with the subscripts 1 and 2 in (2.5) being the breakpoints between adjacent angle points.

The response area at θ_i is obtained from measured channel count rates and monitor detector count rates. For the MAGED electron calibration at the MIT VdeG, the detection area is calculated from

$$A(E,\Omega_i) = (Ct_{Ei} / T_{Ei}) \times (T_M \times A_{Mj} \times (D_T / D_{Mj})^2) / (Ct_{Mj} \times K_{Mj}) \qquad (2.6)$$

where

Ct_{Ei} = the 1ME1 through 1ME5 channel counts

T_{Ei} = the counting time for the 1ME1 through 1ME5 counts (s)

Ct_{Mj} = M1 (or M2) monitor counts

T_M = Monitor count time (s)

A_{Mj} = area of M1 (or M2) monitor (cm^2)

D_T = distance of telescope 1 detector collimator from electron vacuum exit (in)

D_{Mj} = distance of M1 (or M2) monitor detector from electron vacuum exit (in)

K_{Mj} = normalization factor for M1 (or M2) monitor detector to beam center intensity

The values of the last factor are given by

$$K_{M1} = (M2_{\text{in beam}} / M1_{\text{M2 in beam}}) \times (A_{M1} / A_{M2}) \qquad (2.7)$$

and

$$K_{M2} = (M2_{\text{in beam}} / M1_{\text{M2 in beam}}) \times (M1_{\text{M2 out of beam}} / M2_{\text{out of beam}}) \qquad (2.8)$$

The values of (2.7) and (2.8) are generally measured before and after each angle scan set, and the average is used in (2.6).

For the MAGED electron calibration at the GSFC accelerators, only one monitor detector is used, and it is mechanically inserted in front of the MAGED telescope 1 for beam measurements before and after each angle scan set. For this geometry the detection area is calculated from

$$A(E,\Omega_i) = (Ct_{Ei} / T_{Ei}) \times (T_M \times A_M / Ct_M) \qquad (2.9)$$

where

Ct_{Ei} = the 1ME1 through 1ME5 channel counts

T_{Ei} = the counting time for the 1ME1 through 1ME5 counts (s)

Ct_M = monitor counts

T_M = monitor count time (s)

A_M = area of monitor detector = 0.50 cm^2

The MAGED electron calibration at the MIT VdeG used measurement sets in θ_i from 0 deg to 30 deg in 5 deg steps, and a few sets where θ_i varied from –30 deg to +30 deg in 5 deg steps. The sum of (2.4) used the solid angle factors listed in Table 2-1 to calculate the total G(E). For the +θ and -θ measurement sets the two measured area values were averaged for use in (2.4).

The MAGED electron and proton calibration at the GSFC accelerators used measurement sets in θ_i from 0 deg to 15 deg in 5 deg steps, and a few sets where θ_i varied from –15 deg to +15 deg in 5 deg steps. Several scans were made to larger angles, to verify the cut-off at 15 deg. The GSFC measurements are made in vacuum, so there is no scattering of the electrons as in the air path at the MIT VdeG, so the measured angular response at GSFC is narrower than at MIT.

The sum of (2.4) used the solid angle factors listed in Table 2-1 to calculate the total G(E). For the +θ and -θ measurement sets the two measured area values were averaged for use in (2.4).

Table 2-1. Solid Angle Factors ($\Delta\Omega_i$) Values

θ_i (degrees)	θ_2 / θ_1 (degrees)	$\Delta\Omega_i$ (sr)
0	2.5 / 0	0.005980
5	7.5 / 2.5	0.04777
10	12.5 / 7.5	0.09518
15	17.5 / 12.5	0.14187
20	22.5 / 17.5	0.18747
25	27.5 / 22.55	0.23165
30	32.5 / 27.5	0.27407

2.3 Equipment Setup

The basic calibration set-up at the MIT VdeG is shown in Figure 2-2, where the monitor detectors and MAGED locations are shown. The M2 monitor detector is scanned in front of the MAGED to provide corrections for a non-uniform electron beam, using the M1 monitor as a reference. During the MAGED measurements both monitor detectors are used to provide a measure of the electron beam intensity. The air paths to the monitor detectors and to the MAGED are used to correct the electron beam energy for energy loss in the air. The distances to the monitor detector collimators are used to provide electron beam intensity corrections for the beam at the MAGED.

The electronics configuration is shown in Figure 2-3, with a portion of the electronics being located in the electron beam room, and some of the electronics being located in the VdeG control room. The monitor detectors were calibrated with the Compton

edge of a Cs-137 gamma ray source (477 keV), and this was used along with the full energy peak measured by the monitor detectors to calculate the actual electron beam energy. The VdeG exit window was 0.003 inch of aluminum, and this along with the air paths to the monitor detectors was used to calculate a true VdeG beam energy at the exit window. The air path to the telescope 1 detector was then used to calculate an effective electron energy at the detector, which is the energy for the calibration data. The electron beam energy was thus directly calibrated for each energy data set.

The rotating table in Figure 2-2 was used to perform the azimuth angle scans. For most of the energy measurements the azimuth angle scans were 0 degree to 30 degrees in 5 degree steps. Each azimuth scan had the 0 degree azimuth point repeated at the end of the scan to verify measurement stability. For data analysis, the multiple 0 degree azimuth points were averaged for the final area value.

The values for some of the constants in (2.6) for the MAGED calibrations at MIT are given below:

T_{1ME1} = the counting time for the 1ME1 channel counts = 2.048 s

T_{1ME2} = the counting time for the 1ME2 channel counts = 2.048 s

T_{1ME3} = the counting time for the 1ME3 channel counts = 4.096 s

T_{1ME4} = the counting time for the 1ME4 channel counts = 16.384 s

T_{1ME5} = the counting time for the 1ME5 channel counts = 32.768 s

T_M = Monitor count time = 10 s

A_{M1} = area of M1 monitor collimator = 0.1734 cm^2

A_{M2} = area of M2 monitor collimator = 0.2027 cm^2

D_{M1} = distance of M1 monitor detector collimator entrance from electron vacuum exit = 25.0 in

D_{M2} = distance of M2 monitor detector collimator entrance from electron vacuum exit = 23.0 in

D_D = distance of the MAGED telescope 1 detector from electron vacuum exit = 30.25 in

The remaining numbers vary for each individual measurement, although the K_{Mj} values are constant for a given electron energy run. The values of K_{Mj} were measured before and after the angle scans at each energy, and the average values are used for the data analysis. Data were checked for reasonable consistency, to ensure that there are no significant variations in electron beam properties during a particular measurement set. The monitor detectors and 1MEi channel count rates were monitored during the measurements, and the VdeG beam intensity was adjusted to keep the count rates below a level where dead-time effects become important. The VdeG beam occasionally exhibited dark-current pulsations, mostly at the highest energies, and the VdeG had to be "conditioned" at a higher voltage to clean up the beam. Data from such periods was retaken, as necessary, to avoid using data contaminated by high intensity electron/bremsstrahlung background counts.

The electron energy calculations from the monitor detector full energy measurements used the total air path from the VdeG exit window to the detector face, and also included the loss in the 0.3 mil aluminum light shield in front of the monitor detectors. The corrected electron energy at the telescope 1 detector, as calculated from the M1 and M2 monitor detector measurements

separately, generally agreed to better than 2%. Electron energy losses in aluminum and air were calculated using the electron stopping powers in Reference 4.

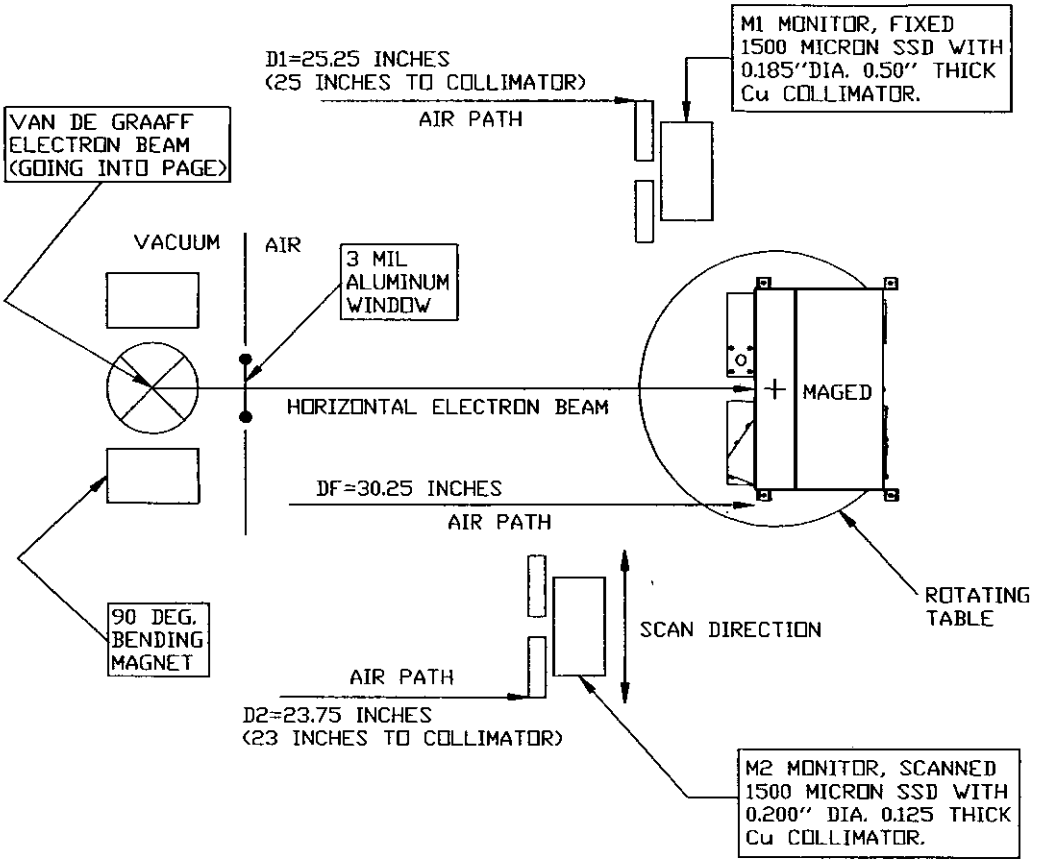

Figure 2-2. Calibration Configuration at MIT Van de Graaff

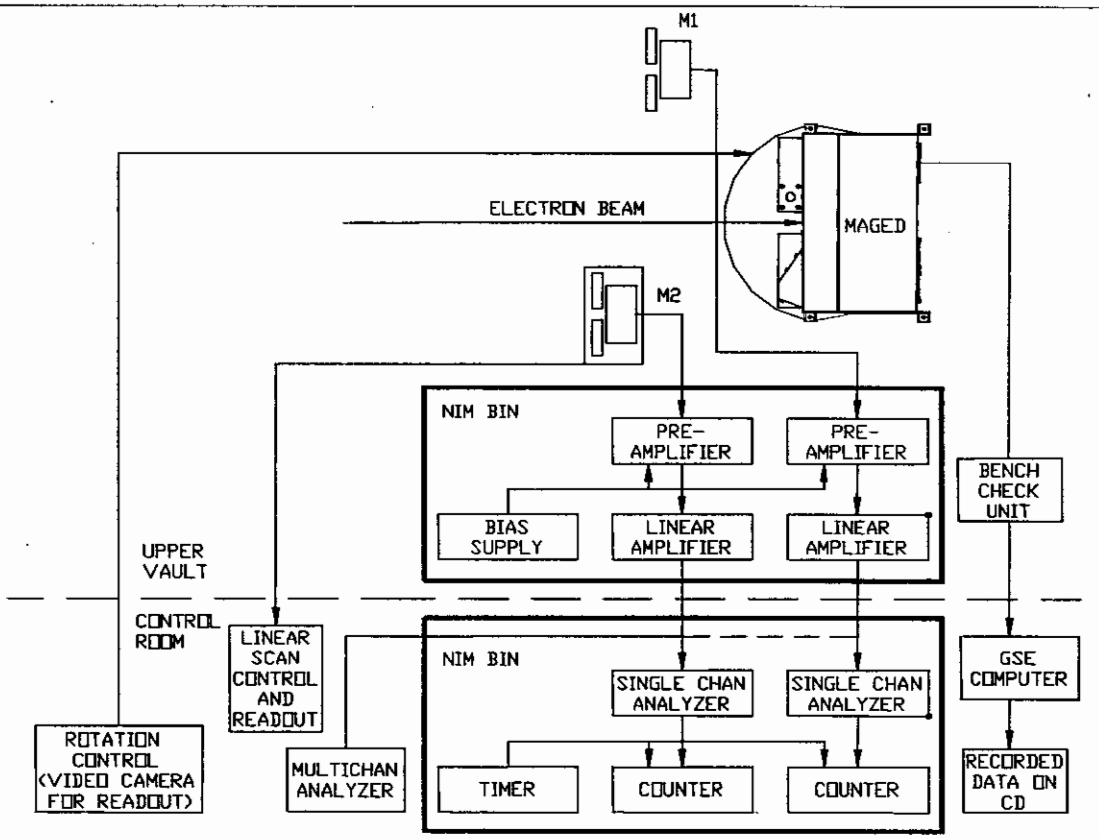

Figure 2-3. Electronics Configuration at MIT Van de Graaff

The basic calibration set-up at the GSFC accelerators is similar to that shown in Figure 2-2 for MIT, except that only one monitor detector is used, and the MAGED and monitor detector are mounted inside a vacuum chamber. The monitor detector is inserted in front of the MAGED before and after each angular scan set to provide beam intensity data. Since the measurements are made in vacuum, the only energy loss corrections to the monitor detector measurements is for energy losses in the 40 ug/cm^2 Au layer and the 0.5 um Si dead layer on the monitor detector front surface. The monitor detector is after the beam collimators, and thus the monitor detector detection area is the full area of the monitor detector, or 50 mm^2.

The electronics configuration is also similar to that shown in Figure 2-3 for MIT, again with only one monitor detector being used. For the low energy calibrations, all equipment was located near the Cockroft-Walton accelerator. For the high energy measurements a portion of the electronics is located in the particle beam room, and some of the electronics is located in the VdeG control room. The monitor detector was calibrated with the Compton edge of a Cs-137 gamma ray source (477 keV) for the low energy easurements, and with the full energy Am-241 alpha particle (5.48 MeV) for the high energy measurements. The monitor detector beam energy measurements were corrected to provide a true beam energy. The particle beam energy was thus directly calibrated for each energy data set.

For the GSFC calibrations, the rotating table in Figure 2-2 was replaced by a rotating vacuum feedthru shaft, which was used to perform the azimuth angle scans. For most of the energy measurements the azimuth angle scans were -15 degrees to +15 degrees in 5 degree steps. Each azimuth scan had the 0 degree azimuth point repeated at the end of the scan to verify measurement stability. For data analysis, the multiple 0 degree azimuth points were averaged for the final area value.

The values for some of the constants in (2.9) for the MAGED calibrations at GSFC are given below.

T_{1ME1} = the counting time for the 1ME1 channel counts = 2.048 s

T_{1ME2} = the counting time for the 1ME2 channel counts = 2.048 s

T_{1ME3} = the counting time for the 1ME3 channel counts = 4.096 s

T_{1ME4} = the counting time for the 1ME4 channel counts = 16.384 s

T_{1ME5} = the counting time for the 1ME5 channel counts = 32.768 s

T_M = Monitor count time = 1 s

A_M = area of monitor detector = 0.500 cm^2

The remaining numbers vary for each individual measurement. Data were checked for reasonable consistency, to ensure that there were no significant variations in electron beam properties during a particular measurement set. The monitor detector and 1MEi channel count rates were monitored during the measurements, and the accelerator beam intensity was adjusted to keep the count rates below a level where dead-time effects become important.

The electron energy calculations from the monitor detector measurements used the electron energy losses in Au and Si from Refs. 4 and 5, while the proton data came from Ref. 6.

3.0 DATA ANALYSIS AND RESULTS

3.1 Measured Detector Areas

3.1.1 1MEi Electron Channel Measured Areas for Electrons at GSFC

The telescope 1 measured 1MEi channel areas for electrons at GSFC for several energies are summarized in Tables 3-1 to 3-14. The calibrated electron energy measured by the GSFC monitor detector is listed for each measurement. The areas are calculated from the monitor detector collimator area, using the procedure described in Section 2.2. Measurements for most electron energies covered the range of 0 deg to 15 deg in 5 deg steps in azimuth, with several energies having both positive and negative azimuth angles measured. A few energies had slightly larger angle sets measured to verify the sharp cut-off at +/-15 deg.

Plots of the measured areas are shown in Figure 3-1 for 1ME2 and 1ME3 at 100 keV, which is at the transition of the response for the two channels, and in Figure 3-2 for 1ME2 at 90 keV, which is well within the 1ME2 response band. Since the measurements are made in vacuum with a very narrow angular spread to the electron beam, the data show the cut-off at +/-15 deg, in agreement with the calculated response.

Table 3-1. Measured 1MEi Detection Areas in cm^2 for 24.0 keV Electrons

Angle (°)	Area (cm^2)				
	1ME1	1ME2	1ME3	1ME4	1ME5
0	1.59E-04	0	0	0	0

Table 3-2. Measured 1MEi Detection Areas in cm^2 for 29.5 keV Electrons

Angle (°)	Area (cm^2)				
	1ME1	1ME2	1ME3	1ME4	1ME5
0	4.60E-03	0	0	0	0
5	5.70E-03	0	0	0	0
10	2.21E-03	0	0	0	0
15	2.12E-04	0	0	0	0
20	0	0	0	0	0
-15	0	0	0	0	0
-10	4.10E-03	0	0	0	0
-5	5.82E-03	0	0	0	0
0	6.35E-03	0	0	0	0

Table 3-3. Measured 1MEi Detection Areas in cm^2 for 34.5 keV Electrons

Angle (°)	Area (cm^2)				
	1ME1	1ME2	1ME3	1ME4	1ME5
0	8.97E-03	0	0	0	0
5	4.80E-03	0	0	0	0
10	2.31E-03	0	0	0	0
15	5.47E-04	0	0	0	0
20	0	0	0	0	0
-15	0	0	0	0	0
-10	9.63E-03	0	0	0	0
-5	1.26E-02	0	0	0	0
0	9.71E-03	0	0	0	0

Table 3-4. Measured 1MEi Detection Areas in cm^2 for 40.4 keV Electrons

Angle (°)	Area (cm^2)				
	1ME1	1ME2	1ME3	1ME4	1ME5
0	3.81E-02	3.81E-05	0	0	0
5	3.52E-02	0	0	0	0
10	1.78E-02	0	0	0	0
15	2.10E-03	0	0	0	0
20	7.51E-05	0	0	0	0
-15	3.40E-03	0	0	0	0
-10	2.58E-02	0	0	0	0
-5	3.81E-02	3.81E-05	0	0	0
0	3.55E-02	0	0	0	0

Table 3-5. Measured 1MEi Detection Areas in cm^2 for 45.0 keV Electrons

Angle (°)	Area (cm^2)				
	1ME1	1ME2	1ME3	1ME4	1ME5
0	2.48E-02	1.78E-04	0	0	0
5	2.43E-02	9.21E-05	0	0	0
10	1.26E-02	4.52E-05	0	0	0
15	3.13E-03	0	0	0	0
20	8.42E-05	0	0	0	0
-10	1.93E-02	1.63E-04	0	0	0
-5	2.58E-02	3.49E-04	0	0	0
0	1.80E-02	4.21E-04	0	0	0

Table 3-6. Measured 1MEi Detection Areas in cm^2 for 50.0 keV Electrons

Angle (°)	Area (cm^2)				
	1ME1	1ME2	1ME3	1ME4	1ME5
0	3.44E-02	1.25E-02	0	0	0
5	2.62E-02	7.85E-03	0	0	0
10	1.69E-02	4.71E-03	0	0	0
15	2.47E-03	1.93E-04	0	0	0
20	9.51E-05	0	0	0	0
-10	1.77E-02	5.42E-03	0	0	0
-5	2.25E-02	7.04E-03	0	0	0
0	2.25E-02	6.67E-03	0	0	0

Table 3-7. Measured 1MEi Detection Areas in cm^2 for 50.0 keV Electrons (Repeat Set)

Angle (°)	Area (cm^2)				
	1ME1	1ME2	1ME3	1ME4	1ME5
0	3.48E-02	1.19E-02	0	0	0
5	2.90E-02	9.99E-03	0	0	0
10	1.66E-02	5.09E-03	0	0	0
0	2.56E-02	8.37E-03	0	0	0

Table 3-8. Measured 1MEi Detection Areas in cm^2 for 55.0 keV Electrons

Angle (°)	Area (cm^2)				
	1ME1	1ME2	1ME3	1ME4	1ME5
0	1.74E-02	5.54E-02	1.11E-05	0	0
5	1.39E-02	4.75E-02	0	0	0
10	1.02E-02	2.56E-02	0	0	0
15	2.95E-03	2.38E-03	0	0	0
20	2.76E-04	1.27E-04	0	0	0
-10	1.13E-02	3.08E-02	1.07E-05	0	0
-5	1.62E-02	5.11E-02	0	0	0
0	1.66E-02	5.03E-02	1.06E-05	0	0

Table 3-9. Measured 1MEi Detection Areas in cm^2 for 60.0 keV Electrons

Angle (°)	Area (cm^2)				
	1ME1	1ME2	1ME3	1ME4	1ME5
0	9.08E-03	6.19E-02	0	0	0
5	8.62E-03	5.88E-02	0	0	0
10	5.49E-03	3.59E-02	0	0	0
15	1.80E-03	4.49E-03	0	0	0
20	1.25E-04	2.19E-04	0	0	0
-10	5.65E-03	3.48E-02	0	0	0
-5	8.78E-03	5.95E-02	5.95E-05	0	0
0	8.03E-03	5.81E-02	0	0	0

Table 3-10. Measured 1MEi Detection Areas in cm^2 for 75.0 keV Electrons

Angle (°)	Area (cm^2)				
	1ME1	1ME2	1ME3	1ME4	1ME5
0	7.97E-03	1.05E-01	0	0	0
5	8.92E-03	8.01E-02	4.21E-05	0	0
10	5.47E-03	5.24E-02	0	0	0
15	2.03E-03	1.15E-02	0	0	0
20	1.68E-04	3.37E-04	0	0	0
0	7.32E-03	9.82E-02	3.94E-05	0	0
-10	9.90E-03	8.88E-02	0	0	0
-5	7.76E-03	7.46E-02	4.36E-05	0	0
0	6.88E-03	8.33E-02	5.55E-05	0	0

Table 3-11. Measured 1MEi Detection Areas in cm^2 for 90.0 keV Electrons

Angle (°)	Area (cm^2)				
	1ME1	1ME2	1ME3	1ME4	1ME5
0	5.88E-03	6.21E-02	0	0	0
5	3.92E-03	5.79E-02	0	0	0
10	2.69E-03	3.02E-02	0	0	0
15	1.02E-03	8.82E-03	0	0	0
20	0	8.37E-04	0	0	0
-10	4.70E-03	5.85E-02	0	0	0
-5	6.85E-03	7.35E-02	4.70E-05	0	0
0	6.60E-03	8.17E-02	9.04E-05	0	0

Table 3-12. Measured 1MEi Detection Areas in cm^2 for 100.0 keV Electrons

Angle (°)	Area (cm^2)				
	1ME1	1ME2	1ME3	1ME4	1ME5
0	7.60E-03	4.22E-02	5.10E-02	0	0
5	7.32E-03	3.74E-02	5.67E-02	0	0
10	5.70E-03	2.77E-02	3.52E-02	0	0
15	1.14E-03	6.48E-03	2.78E-03	0	0
20	1.48E-04	5.92E-04	1.11E-04	0	0
25	0	0	0	0	0
-20	0	0	0	0	0
-15	5.28E-04	1.52E-03	2.97E-04	0	0
-10	3.21E-03	1.69E-02	1.90E-02	0	0
-5	5.51E-03	3.07E-02	5.48E-02	0	0
0	9.28E-03	4.64E-02	6.42E-02	0	0

Table 3-13. Measured E1 Detection Areas in cm^2 for 115.0 keV Electrons

Angle (°)	Area (cm^2)				
	1ME1	1ME2	1ME3	1ME4	1ME5
0	8.87E-03	1.52E-02	1.22E-01	3.73E-05	0
5	7.13E-03	1.29E-02	9.81E-02	2.03E-05	0
10	5.50E-03	8.68E-03	5.60E-02	7.35E-06	0
15	8.23E-04	2.55E-03	6.19E-03	0	0
20	0	1.48E-04	4.69E-04	0	0
25	0	0	0	0	0
-15	3.60E-04	8.22E-04	1.79E-03	3.21E-06	0
-10	2.59E-03	4.76E-03	3.36E-02	0	0
-5	4.48E-03	7.06E-03	5.67E-02	1.50E-05	0
0	3.59E-03	7.59E-03	5.47E-02	1.83E-05	0

Table 3-14. Measured E1 Detection Areas in cm^2 for 115.0 keV Electrons (Repeat Set)

Angle (°)	Area (cm^2)				
	1ME1	1ME2	1ME3	1ME4	1ME5
0	1.06E-02	1.86E-02	1.56E-01	2.37E-05	0
-10	5.47E-03	9.64E-03	7.07E-02	1.93E-05	0
0	7.37E-03	1.41E-02	1.08E-01	2.31E-05	0
10	4.00E-03	8.40E-03	5.24E-02	2.92E-06	0

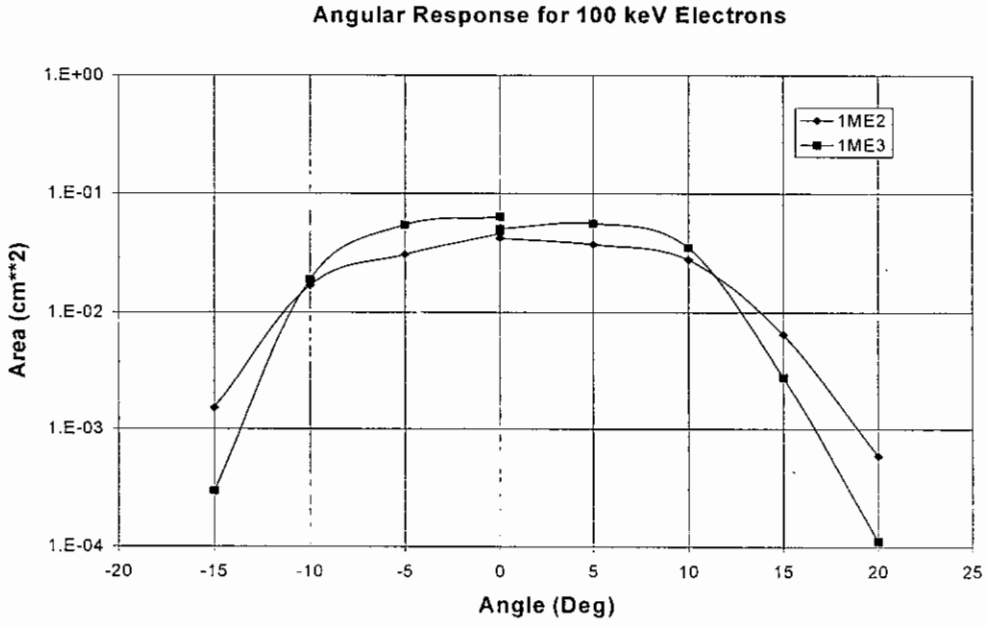

Figure 3-1. Angular Response of 1ME2 and 1ME3 at 100 keV

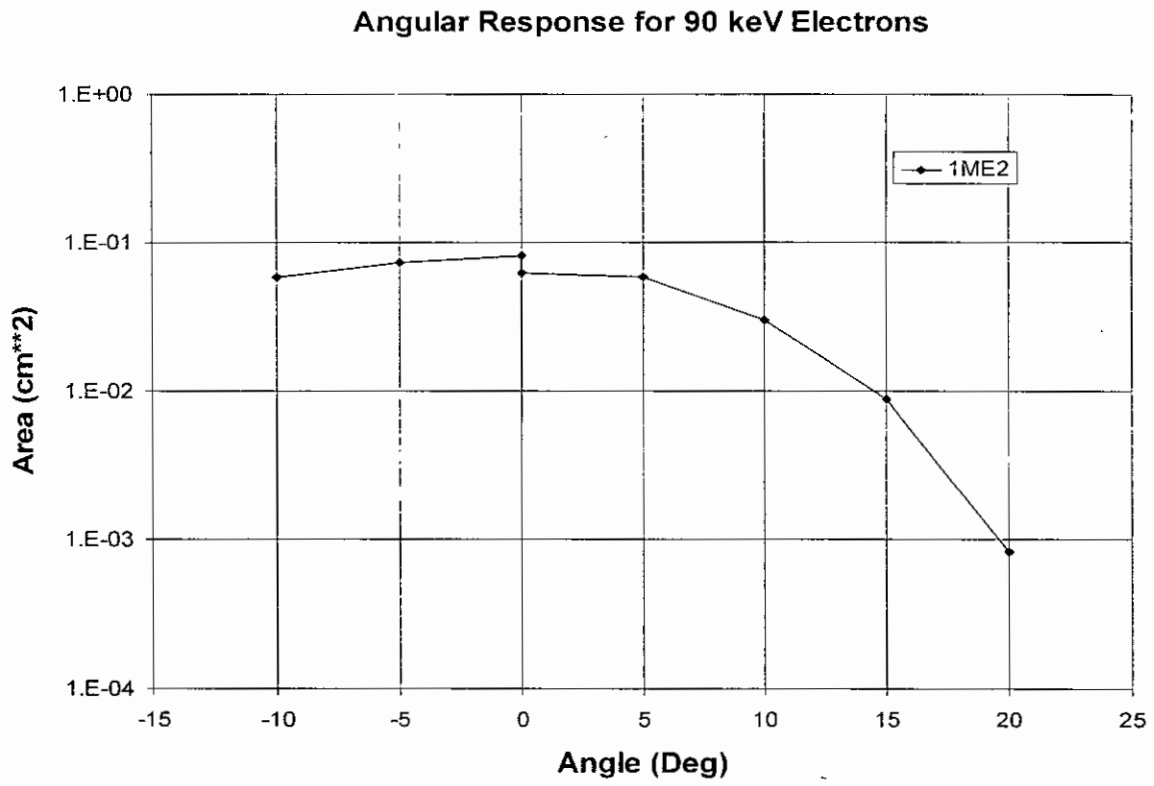

Figure 3-2. Angular Response of 1ME2 at 90 keV

3.1.2 1MEi Electron Channel Measured Areas for Electrons at MIT

The telescope 1 measured 1MEi channel areas for electrons at several energies are summarized in Tables 3-15 to 3-29. The calibrated electron energy at the telescope 1 detector is listed for each measurement. The areas are calculated from the two monitor detector collimator areas, using the procedure described in Section 2.2. Measurements for most electron energies covered the range of 0 deg to 30 deg in 5 deg steps in azimuth, with several energies having both positive and negative azimuth angles measured.

A plot of the measured areas is shown in Figure 3-3 for 1ME4 and 1ME5 at 398 keV, which is near the transition energy from 1ME4 to 1ME5. The measurements at the MIT VdeG are made in air, with the electron beam exiting vacuum through a 3 mil Al foil, so there is significant scattering of the electron beam, which broadens the beam angular distribution. Thus the MIT calibrations show a significantly wider angular response for the electron channels. The actual channel response is a cut-off at +/- 15 deg, as shown by the GSFC data taken in vacuum (Section 3.1.1).

Table 3-15. Measured 1MEi Detection Areas in cm^2 for 114 keV Electrons

Angle (°)	Area (cm^2)				
	1ME1	1ME2	1ME3	1ME4	1ME5
0	2.53E-02	2.43E-02	7.28E-03	3.64E-04	0
5	3.52E-02	3.27E-02	1.64E-02	4.55E-04	0
10	2.31E-02	2.69E-02	8.66E-03	2.16E-03	0
15	8.61E-03	1.86E-02	4.30E-03	3.59E-04	0
20	1.35E-02	1.50E-02	2.25E-03	1.87E-04	0
25	1.33E-02	2.10E-02	1.24E-02	4.77E-04	0
30	2.72E-03	2.44E-02	5.43E-03	1.02E-03	8.49E-05
0	4.48E-02	4.04E-02	2.47E-02	2.80E-04	0
-5	3.87E-02	2.95E-02	1.01E-02	4.61E-04	0
-10	3.92E-02	2.04E-02	1.26E-02	1.96E-04	0
-15	9.99E-03	1.28E-02	1.21E-02	3.57E-04	0
-20	7.33E-03	1.61E-02	6.59E-03	1.83E-04	9.16E-05
-25	2.14E-03	1.49E-02	4.27E-03	2.67E-04	0
-30	4.73E-03	7.09E-03	4.14E-03	2.95E-04	0
0	1.95E-02	3.20E-02	1.25E-02	1.74E-04	0

Table 3-16. Measured 1MEi Detection Areas in cm^2 for 168 keV Electrons

Angle (°)	Area (cm^2)				
	1ME1	1ME2	1ME3	1ME4	1ME5
0	6.28E-03	6.28E-03	1.57E-02	3.93E-03	0
5	8.45E-03	5.64E-03	1.63E-02	2.42E-03	0
10	3.57E-03	5.58E-03	1.39E-02	2.50E-03	6.98E-06
15	1.94E-03	4.97E-03	1.10E-02	1.98E-03	0
20	2.22E-03	3.63E-03	1.10E-02	1.48E-03	0
25	2.15E-03	5.71E-03	9.64E-03	1.43E-03	0
30	2.06E-03	4.13E-03	7.51E-03	1.05E-03	0
0	7.07E-03	6.12E-03	1.24E-02	3.41E-03	9.93E-06

Table 3-17. Measured 1MEi Detection Areas in cm^2 for 261 keV Electrons

Angle (°)	Area (cm^2)				
	1ME1	1ME2	1ME3	1ME4	1ME5
0	2.54E-03	4.44E-03	1.29E-02	2.22E-02	9.92E-06
5	1.13E-03	2.99E-03	8.32E-03	2.21E-02	3.52E-06
10	6.50E-04	2.47E-03	9.04E-03	2.03E-02	0
15	4.34E-04	8.68E-04	2.75E-03	1.55E-02	0
20	7.94E-04	1.59E-03	6.43E-03	1.36E-02	0
25	6.19E-04	9.28E-04	2.78E-03	1.21E-02	0
30	3.71E-04	1.11E-03	3.90E-03	7.94E-03	0
0	2.61E-03	4.06E-03	1.00E-02	2.84E-02	0
-5	8.69E-04	2.85E-03	7.70E-03	2.13E-02	7.76E-06

Table 3-18. Measured 1MEi Detection Areas in cm^2 for 341 keV Electrons

Angle (°)	Area (cm^2)				
	1ME1	1ME2	1ME3	1ME4	1ME5
0	8.42E-04	2.02E-03	4.21E-03	2.76E-02	3.10E-03
5	7.22E-04	2.35E-03	4.78E-03	2.81E-02	2.11E-03
10	1.24E-03	8.88E-04	4.44E-03	2.34E-02	2.36E-03
15	6.93E-04	2.60E-03	5.37E-03	2.06E-02	1.50E-03
20	3.74E-04	2.37E-03	2.87E-03	1.56E-02	1.15E-03
25	1.29E-04	5.16E-04	1.61E-03	1.21E-02	9.02E-04
30	0	4.27E-04	2.35E-03	1.94E-02	4.80E-04
35	4.37E-04	1.31E-03	1.31E-03	7.18E-03	2.19E-04
0	5.19E-04	7.79E-04	5.45E-03	2.93E-02	3.46E-03

Table 3-19. Measured 1MEi Detection Areas in cm^2 for 398 keV Electrons

Angle (°)	Area (cm^2)				
	1ME1	1ME2	1ME3	1ME4	1ME5
0	6.23E-04	2.49E-03	3.43E-03	1.52E-02	2.43E-02
5	9.93E-04	1.99E-03	4.47E-03	1.44E-02	2.18E-02
10	0	2.47E-03	4.94E-03	1.40E-02	1.89E-02
15	1.19E-03	1.19E-03	3.77E-03	9.68E-03	1.39E-02
20	4.05E-04	4.05E-04	2.63E-03	8.25E-03	9.89E-03
25	0	8.50E-04	3.61E-03	6.27E-03	5.66E-03
30	0	1.80E-03	1.12E-03	4.78E-03	3.91E-03
0	0	2.34E-03	5.15E-03	1.46E-02	2.29E-02
-5	0	2.39E-03	4.53E-03	1.34E-02	2.24E-02
-10	9.44E-04	2.83E-03	6.61E-03	1.28E-02	1.74E-02
-15	0	1.49E-03	4.47E-03	1.10E-02	1.48E-02
-20	1.08E-03	1.08E-03	3.59E-03	9.55E-03	1.18E-02
-25	0	2.09E-03	3.31E-03	8.15E-03	1.09E-02
-30	3.42E-04	1.71E-03	1.71E-03	9.63E-03	8.71E-03
0	6.75E-04	1.01E-03	5.23E-03	1.46E-02	2.23E-02

Table 3-20. Measured 1MEi Detection Areas in cm^2 for 520 keV Electrons

Angle (°)	Area (cm^2)				
	1ME1	1ME2	1ME3	1ME4	1ME5
0	5.94E-04	1.45E-03	3.70E-03	7.06E-03	3.91E-02
5	1.00E-03	1.37E-03	3.66E-03	7.36E-03	3.79E-02
10	4.53E-04	6.04E-04	2.76E-03	5.28E-03	3.08E-02
15	1.32E-04	5.93E-04	1.58E-03	4.34E-03	1.95E-02
20	2.98E-04	5.22E-04	1.79E-03	2.75E-03	1.28E-02
25	2.56E-04	4.26E-04	1.15E-03	1.74E-03	7.32E-03
30	1.64E-04	8.18E-05	5.72E-04	9.91E-04	4.00E-03
0	5.29E-04	2.03E-03	3.39E-03	7.57E-03	3.77E-02

Table 3-21. Measured 1MEi Detection Areas in cm^2 for 639 keV Electrons

Angle (°)	Area (cm^2)				
	1ME1	1ME2	1ME3	1ME4	1ME5
0	1.26E-03	1.63E-03	2.89E-03	9.85E-03	2.46E-02
5	6.29E-04	8.81E-04	2.27E-03	1.03E-02	2.47E-02
10	7.39E-04	6.16E-04	2.96E-03	7.69E-03	2.02E-02
15	4.96E-04	6.20E-04	1.30E-03	4.82E-03	1.33E-02
20	1.28E-04	2.55E-04	1.15E-03	2.98E-03	7.21E-03
25	2.63E-04	2.63E-04	7.90E-04	1.46E-03	3.91E-03
30	2.86E-04	0	7.86E-04	7.50E-04	2.35E-03
0	4.55E-04	7.58E-04	2.05E-03	9.99E-03	2.61E-02

Table 3-22. Measured 1MEi Detection Areas in cm^2 for 750 keV Electrons

Angle (°)	Area (cm^2)				
	1ME1	1ME2	1ME3	1ME4	1ME5
0	6.06E-04	1.46E-03	2.30E-03	1.60E-02	1.89E-02
5	8.68E-04	1.49E-03	2.98E-03	1.47E-02	1.83E-02
10	2.41E-04	1.44E-03	2.29E-03	1.13E-02	1.43E-02
15	4.91E-04	2.45E-04	1.84E-03	7.28E-03	9.56E-03
20	0	5.01E-04	6.26E-04	4.12E-03	4.91E-03
25	0	5.64E-04	4.23E-04	1.87E-03	2.19E-03
30	0	1.35E-04	2.03E-04	1.17E-03	1.18E-03
0	1.16E-03	8.27E-04	3.97E-03	1.55E-02	1.97E-02

Table 3-23. Measured 1MEi Detection Areas in cm^2 for 813 keV Electrons

Angle (°)	Area (cm^2)				
	1ME1	1ME2	1ME3	1ME4	1ME5
0	8.25E-04	1.18E-03	2.71E-03	2.03E-02	1.92E-02
5	6.81E-04	1.13E-03	3.35E-03	1.95E-02	1.77E-02
10	5.52E-04	1.10E-03	2.65E-03	1.46E-02	1.46E-02
15	2.10E-04	6.29E-04	9.96E-04	9.00E-03	8.17E-03
20	3.47E-04	5.78E-04	8.67E-04	4.49E-03	4.50E-03
25	1.27E-04	1.27E-04	6.36E-04	1.78E-03	2.09E-03
30	1.53E-04	1.53E-04	1.53E-04	6.49E-04	1.01E-03
0	7.67E-04	1.07E-03	1.76E-03	1.92E-02	1.82E-02

Table 3-24. Measured 1MEi Detection Areas in cm^2 for 869 keV Electrons

Angle (°)	Area (cm^2)				
	1ME1	1ME2	1ME3	1ME4	1ME5
0	1.49E-03	1.49E-03	2.61E-03	2.32E-02	2.10E-02
5	1.36E-03	1.70E-03	2.71E-03	2.24E-02	1.81E-02
10	6.33E-04	1.58E-03	5.06E-03	1.78E-02	1.49E-02
15	0	9.11E-04	1.14E-03	1.11E-02	8.85E-03
20	0	0	1.25E-03	5.79E-03	4.55E-03
25	0	0	5.45E-04	1.98E-03	1.57E-03
30	0	0	0	0	0
0	1.15E-03	1.15E-03	3.46E-03	2.28E-02	1.88E-02

Table 3-25. Measured 1MEi Detection Areas in cm^2 for 932 keV Electrons

Angle (°)	Area (cm^2)				
	1ME1	1ME2	1ME3	1ME4	1ME5
0	1.03E-03	1.45E-03	2.69E-03	2.21E-02	1.69E-02
5	2.26E-04	1.58E-03	2.60E-03	2.83E-02	2.04E-02
10	8.36E-04	1.25E-03	3.24E-03	2.04E-02	1.38E-02
15	5.39E-04	5.39E-04	2.25E-03	1.26E-02	8.80E-03
20	0	3.90E-04	7.79E-04	4.75E-03	4.76E-03
25	0	2.04E-04	5.11E-04	2.17E-03	2.08E-03
30	0	0	3.36E-04	7.83E-04	7.83E-04
0	8.30E-04	6.22E-04	3.53E-03	2.34E-02	1.78E-02

Table 3-26. Measured 1MEi Detection Areas in cm^2 for 997 keV Electrons

Angle (°)	Area (cm^2)				
	1ME1	1ME2	1ME3	1ME4	1ME5
0	9.69E-04	1.61E-03	3.27E-03	2.78E-02	2.02E-02
5	7.59E-04	1.21E-03	2.73E-03	2.49E-02	1.71E-02
10	5.44E-04	1.81E-03	2.00E-03	2.16E-02	1.34E-02
15	2.05E-04	6.15E-04	6.15E-04	1.28E-02	7.17E-03
20	0	2.55E-04	5.10E-04	4.68E-03	3.39E-03
25	0	0	5.19E-04	1.30E-03	1.15E-03
30	0	0	0	6.08E-04	6.08E-04
0	9.92E-04	2.32E-03	3.97E-03	3.37E-02	1.97E-02
-5	1.37E-03	1.65E-03	3.57E-03	2.47E-02	1.71E-02
-10	0	8.00E-04	2.67E-03	1.76E-02	1.09E-02
-15	2.48E-04	4.96E-04	1.12E-03	8.65E-03	5.56E-03
-20	0	0	4.54E-04	3.52E-03	2.63E-03
-25	0	3.65E-04	3.65E-04	2.19E-03	1.14E-03
-30	0	0	1.35E-04	1.15E-03	1.10E-03
0	6.73E-04	1.01E-03	3.53E-03	2.75E-02	1.80E-02

Table 3-27. Measured 1MEi Detection Areas in cm^2 for 1251 keV Electrons

Angle (°)	Area (cm^2)				
	1ME1	1ME2	1ME3	1ME4	1ME5
0	6.22E-04	2.18E-03	4.35E-03	3.32E-02	1.66E-02
5	1.01E-03	1.01E-03	3.69E-03	3.28E-02	1.71E-02
10	3.30E-04	1.65E-03	3.47E-03	1.96E-02	1.09E-02
15	1.46E-03	0	2.92E-03	9.22E-03	5.98E-03
20	0	0	3.49E-04	4.19E-03	1.49E-03
25	0	0	3.08E-04	1.62E-03	5.77E-04
30	6.07E-04	6.07E-04	3.04E-04	3.80E-04	4.93E-04
0	0	6.57E-04	5.92E-03	3.34E-02	1.54E-02

Table 3-28. Measured 1MEi Detection Areas in cm^2 for 1515 keV Electrons

Angle (°)	Area (cm^2)				
	1ME1	1ME2	1ME3	1ME4	1ME5
0	3.63E-04	2.18E-03	1.02E-02	5.37E-02	2.39E-02
5	1.11E-03	9.29E-04	4.83E-03	3.97E-02	1.99E-02
10	3.75E-04	7.51E-04	2.81E-03	1.91E-02	7.67E-03
15	0	3.85E-04	1.54E-03	1.03E-02	4.70E-03
20	0	2.89E-04	1.01E-03	4.05E-03	2.10E-03
25	0	0	0	1.21E-03	1.24E-03
30	0	0	2.45E-04	4.09E-04	4.09E-04
0	7.54E-04	9.43E-04	8.39E-03	5.28E-02	2.24E-02
-5	9.26E-04	7.41E-04	6.02E-03	4.63E-02	2.09E-02
-10	1.31E-03	1.87E-03	6.07E-03	3.06E-02	1.38E-02
-15	5.01E-04	1.00E-03	7.76E-03	3.90E-02	1.75E-02
-20	3.60E-04	1.80E-04	1.26E-03	5.06E-03	2.01E-03
-25	2.25E-04	4.50E-04	7.87E-04	9.55E-04	6.46E-04
-30	0	0	2.32E-04	2.90E-04	3.19E-04
0	7.79E-04	1.95E-03	6.04E-03	3.97E-02	1.67E-02

Table 3-29. Measured 1MEi Detection Areas in cm^2 for 1724 keV Electrons

Angle (°)	Area (cm^2)				
	1ME1	1ME2	1ME3	1ME4	1ME5
0	9.15E-04	1.83E-03	7.77E-03	4.29E-02	1.36E-02
5	1.35E-03	1.35E-03	5.07E-03	4.22E-02	1.59E-02
10	6.25E-04	6.25E-04	5.63E-03	3.34E-02	1.15E-02
15	2.80E-04	1.19E-03	3.12E-03	8.74E-03	2.31E-03
20	3.75E-04	5.89E-04	2.08E-03	5.46E-03	2.19E-03
25	0	0	2.97E-04	1.15E-03	5.94E-04
25	4.53E-05	4.53E-05	1.58E-04	9.67E-04	5.06E-04
30	9.64E-05	9.64E-05	9.64E-05	3.49E-04	2.65E-04

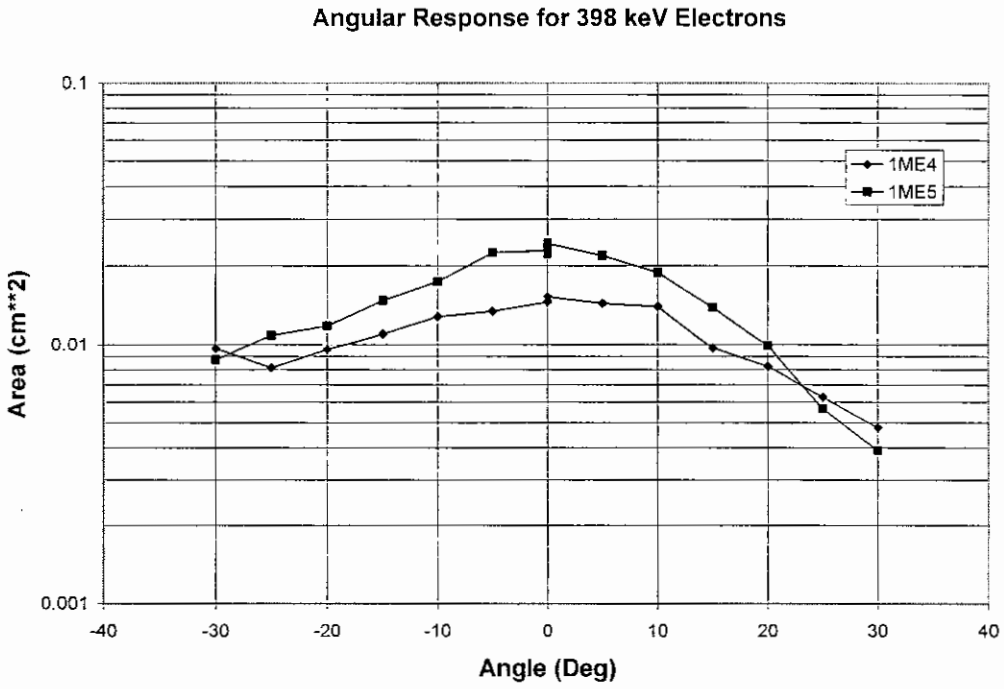

Figure 3-3. Angular Response of 1ME4 and 1ME5 at 398 keV

3.1.3 1MEi Electron Channel Measured Areas for Protons at GSFC

The telescope 1 measured 1MEi channel areas for protons at several energies are summarized in Tables 3-30 to 3-42. The calibrated proton energy from the GSFC monitor detector is listed for each measurement. The areas are calculated from the monitor detector area, using the procedure described in Section 2.2. Measurements for most proton energies covered the range of 0 deg to 15 deg in 5 deg steps in azimuth, with several energies having both positive and negative azimuth angles measured. The last Table 3-42 contains measurements for a number of miscellaneous energies, where only the 0 degree data were taken to provide a more detailed measurement of channel edge energies. Some energies were repeated to provide an estimate of beam stability.

Table 3-30. Measured 1MEi Detection Areas in cm^2 for 208 keV Protons

Angle (°)	Area (cm^2)				
	1ME1	1ME2	1ME3	1ME4	1ME5
0	3.76E-02	4.73E-02	0	0	0
5	2.62E-02	3.34E-02	3.35E-05	0	0
10	1.54E-02	1.72E-02	0	0	0
15	0	0	0	0	0
0	2.98E-02	4.30E-02	3.13E-05	0	0

Table 3-31. Measured 1MEi Detection Areas in cm^2 for 228 keV Protons

Angle (°)	Area (cm^2)				
	1ME1	1ME2	1ME3	1ME4	1ME5
0	6.51E-03	3.66E-02	1.06E-03	2.03E-05	0
5	4.88E-03	3.86E-02	8.95E-04	0	0
10	4.07E-03	2.13E-02	4.88E-04	0	0
15	0	0	0	0	0
0	7.38E-03	4.62E-02	1.09E-03	0	0

Table 3-32. Measured 1MEi Detection Areas in cm^2 for 246 keV Protons

Angle (°)	Area (cm^2)				
	1ME1	1ME2	1ME3	1ME4	1ME5
0	2.03E-03	5.09E-02	1.44E-02	0	0
5	1.90E-03	5.09E-02	1.16E-02	0	0
10	1.36E-03	2.89E-02	6.31E-03	0	0
15	1.36E-04	1.36E-04	6.78E-05	0	8.48E-06
0	1.54E-03	4.79E-02	1.25E-02	0	0

Table 3-33. Measured 1MEi Detection Areas in cm^2 for 292 keV Protons

Angle (°)	Area (cm^2)				
	1ME1	1ME2	1ME3	1ME4	1ME5
0	1.20E-03	3.09E-03	9.07E-02	4.30E-05	0
5	9.59E-04	2.62E-03	7.11E-02	0	0
10	3.37E-04	1.60E-03	3.80E-02	1.05E-05	0
15	9.04E-05	9.04E-05	4.52E-04	0	0
0	1.12E-03	2.71E-03	5.89E-02	1.47E-05	0
-5	7.99E-04	2.84E-03	9.37E-02	1.11E-05	0
-10	6.98E-04	2.39E-03	5.90E-02	0	0
-15	0	0	0	0	0

Table 3-34. Measured 1MEi Detection Areas in cm^2 for 394 keV Protons

Angle (°)	Area (cm^2)				
	1ME1	1ME2	1ME3	1ME4	1ME5
0	2.98E-04	4.17E-04	8.04E-04	1.07E-02	3.72E-06
5	2.36E-04	2.36E-04	3.53E-04	9.18E-03	0
10	0	2.74E-04	1.65E-04	4.27E-03	0
15	0	5.68E-05	2.84E-05	1.42E-05	0
0	2.87E-04	3.45E-04	7.18E-04	1.23E-02	0

Table 3-35. Measured 1MEi Detection Areas in cm^2 for 404 keV Protons

Angle (°)	Area (cm^2)				
	1ME1	1ME2	1ME3	1ME4	1ME5
0	1.75E-04	6.98E-04	2.10E-03	9.78E-02	1.64E-05
5	3.56E-04	7.12E-04	1.16E-03	5.27E-02	0
10	6.23E-04	7.12E-04	8.01E-04	2.92E-02	0
15	1.66E-04	1.66E-04	2.07E-04	3.10E-05	0
0	5.15E-04	9.45E-04	3.31E-03	1.35E-01	1.61E-05
-5	1.66E-04	8.28E-04	2.44E-03	1.96E-01	5.17E-05
-10	0	4.30E-04	1.98E-03	1.72E-01	3.76E-05
-15	0	0	0	7.52E-04	0

Table 3-36. Measured 1MEi Detection Areas in cm^2 for 604 keV Protons

Angle (°)	Area (cm^2)				
	1ME1	1ME2	1ME3	1ME4	1ME5
0	1.14E-04	1.48E-03	1.82E-03	3.96E-03	4.63E-02
5	2.33E-04	4.65E-04	1.86E-03	2.72E-03	4.00E-02
10	3.45E-04	4.60E-04	9.19E-04	5.75E-04	6.83E-03
15	0	0	0	2.47E-04	1.60E-04
0	2.33E-04	1.16E-03	2.79E-03	3.44E-03	3.44E-02
-5	2.33E-04	9.30E-04	1.74E-03	3.82E-03	7.25E-02
-10	0	1.16E-04	2.33E-04	2.62E-04	3.81E-02
-15	0	0	0	0	1.42E-05

Table 3-37. Measured 1MEi Detection Areas in cm^2 for 607 keV Protons

Angle (°)	Area (cm^2)				
	1ME1	1ME2	1ME3	1ME4	1ME5
0	1.63E-04	1.63E-04	4.61E-04	9.43E-04	9.77E-03
5	1.11E-04	1.11E-04	6.94E-04	5.62E-04	3.88E-03
10	0	1.10E-04	2.19E-04	3.43E-04	2.03E-03
15	0	0	8.14E-05	1.36E-04	1.02E-05
0	3.33E-04	6.10E-04	8.60E-04	1.41E-03	1.04E-02

Table 3-38. Measured 1MEi Detection Areas in cm^2 for 608 keV Protons

Angle (°)	Area (cm^2)				
	1ME1	1ME2	1ME3	1ME4	1ME5
0	6.37E-04	7.08E-04	1.13E-03	1.44E-03	2.66E-02
5	3.08E-04	6.92E-04	1.08E-03	2.05E-03	3.48E-02
10	1.50E-04	3.76E-04	7.14E-04	9.11E-04	2.10E-02
15	0	0	0	1.86E-05	5.13E-05
0	2.29E-04	6.87E-04	1.22E-03	1.94E-03	3.11E-02
-5	2.25E-04	6.76E-04	1.20E-03	1.53E-03	2.58E-02
-10	3.01E-04	4.51E-04	1.05E-03	9.96E-04	1.88E-02
-15	0	0	7.46E-05	5.59E-05	1.86E-05
0	6.01E-04	6.01E-04	1.20E-03	1.83E-03	3.07E-02

Table 3-39. Measured 1MEi Detection Areas in cm^2 for 790 keV Protons

Angle (°)	Area (cm^2)				
	1ME1	1ME2	1ME3	1ME4	1ME5
0	4.81E-04	4.81E-04	1.38E-03	2.26E-03	3.37E-03
5	6.88E-04	5.50E-04	7.57E-04	1.61E-03	1.61E-03
10	1.40E-04	1.40E-04	2.79E-04	5.67E-04	6.41E-04
15	0	6.98E-05	3.84E-04	1.83E-04	1.48E-04
0	3.49E-04	3.49E-04	1.08E-03	2.71E-03	3.27E-03

Table 3-40. Measured 1MEi Detection Areas in cm^2 for 795 keV Protons

Angle (°)	Area (cm^2)				
	1ME1	1ME2	1ME3	1ME4	1ME5
0	3.78E-03	8.59E-04	1.63E-03	2.82E-03	4.03E-03
5	2.27E-03	4.21E-04	1.60E-03	2.49E-03	3.28E-03
10	2.06E-03	8.57E-04	1.16E-03	1.66E-03	2.09E-03
15	8.57E-05	2.57E-04	1.29E-04	3.43E-04	4.34E-04
-15	0	9.58E-05	2.39E-04	3.47E-04	4.13E-04
-10	1.63E-03	6.86E-04	9.43E-04	1.49E-03	1.67E-03
-5	3.70E-03	5.28E-04	1.32E-03	2.34E-03	3.60E-03
0	2.88E-03	5.58E-04	1.58E-03	3.24E-03	4.55E-03

Table 3-41. Measured 1MEi Detection Areas in cm^2 for 1052 keV Protons

Angle (°)	Area (cm^2)				
	1ME1	1ME2	1ME3	1ME4	1ME5
0	7.43E-05	8.17E-04	1.49E-03	2.74E-03	5.19E-03
5	2.25E-04	8.27E-04	1.28E-03	1.91E-03	4.02E-03
10	7.75E-05	3.88E-04	6.98E-04	1.09E-03	1.89E-03
15	0	7.88E-05	7.88E-05	1.48E-04	2.17E-04
-15	0	0	7.82E-05	2.15E-04	2.05E-04
-10	4.88E-04	3.26E-04	8.14E-04	1.03E-03	1.58E-03
-5	4.77E-04	8.74E-04	1.51E-03	2.23E-03	4.05E-03
0	3.94E-04	9.45E-04	1.42E-03	2.75E-03	5.51E-03

Table 3-42. Measured 1MEi Detection Areas in cm^2 for Miscellaneous Energy Protons at 0 Degrees

Energy (keV)	Area (cm^2)				
	1ME1	1ME2	1ME3	1ME4	1ME5
273	1.43E-03	2.50E-02	1.06E-01	5.60E-05	2.80E-06
181	2.00E-02	3.88E-03	0	0	0
181	2.54E-02	2.96E-03	0	0	0
159	3.83E-03	9.58E-05	0	0	0
896	5.03E-04	2.87E-04	4.67E-04	1.32E-03	2.37E-03

3.2 Measured Geometric Factors

3.2.1 Electron Geometric Factors

The measured electron geometric factors, obtained by integrating over the angular measurements given in Tables 3-1 through 3-29, and the average A(0) area values, for all 1MEi channels, are summarized in Tables 3-43 through 3-46. The low energy GSFC measurements from Section 3.1.1 are in Tables 3-43 (Gf) and 3-44 (A), while the high energy MIT measurements from Section 3.1.2 are in Tables 3-45 (Gf) and 3-46 (A). The total geometric factor in Tables 3-43 and 3-45 is the sum of the five channel geometric factors.

The MAGED electron telescope design is identical to the TIROS/NOAA SEM-2 MEPED Electron Telescope, except that the MEPED electron telescope uses three integral energy loss channels to provide three integral electron channels for >30 keV (0E1 and 9E1), >100 keV (0E2 and 9E2), and >300 keV (0E3 and 9E3). The >30 keV channels (0E1 and 9E1) should have a response identical to the total geometric factor for the MAGED telescopes. The MEPED electron telescopes were calibrated at the GSFC accelerators, and at a full angle scanning calibration chamber at the Air Force Phillips Laboratory at Hanscom AFB, MA. The calibration of the PM MEPED was reported in Ref. 2, and was performed according to the Test Procedure in Ref. 3. The GSFC electron calibration results for 0E1 and 0E2 are given in Table 3-47, while the 9E1 and 9E2 results are in Table 3-48. The PL calibration results for 0E1 and 9E1 are given in Table 3-49.

The results for the GSFC Gf(E) and A(E,0) are shown in Figures 3-4 and 3-5, while the MIT results are plotted in Figures 3-6 and 3-7. The previous electron calibration data from Ref. 2 are shown in Figures 3-8 (Gf) and 3-9 (A(0)), along with the 1ME1 and total Gf measurements from GSFC. The present measurements are in good agreement with the previous MEPED calibrations, as shown by the closeness of the present total GF and the MEPED 0E1 and 9E1 calibrations, in both Gf and A(0).

Note that the PL low energy calibrations show a higher Gf and A(0) than the GSFC data. This is caused by the PL chamber having a large set of Helmholtz coils to null out the earth's magnetic field, while the GSFC low energy accelerator does not have Helmholtz coils. The lowest energy GSFC electron calibrations have a significant bending of the electron beam, as shown by the fact that in order to see the electron beam the MAGED had to be lowered for the lowest energy measurements. The lowest energy Gf values are thus given best by the PL data, which show a faster rise at 30 keV, and reach the calculated value of 0.0100 cm^2-sr very quickly.

Table 3-43. Measured 1MEi and Total Geometric Factors for Electrons at GSFC

Electron Energy (keV)	Gf(E) (cm2-sr)				
	1ME1	1ME2	1ME3	1ME4	Total
24.0	9.49E-07	0	0	0	9.49E-07
29.5	6.23E-04	0	0	0	6.23E-04
34.5	2.10E-03	0	0	0	2.10E-03
40	4.44E-03	1.03E-06	0	0	4.45E-03
45	6.02E-03	4.26E-05	0	0	6.06E-03
50	3.15E-03	1.02E-03	0	0	4.17E-03
50	3.17E-03	9.09E-04	0	0	4.08E-03
55	2.08E-03	5.54E-03	5.75E-07	0	7.62E-03
60	1.14E-03	6.89E-03	1.42E-06	0	8.03E-03
75	1.33E-03	1.18E-02	2.24E-06	0	1.32E-02
90	7.19E-04	8.50E-03	1.39E-06	0	9.22E-03
100	9.13E-04	4.64E-03	5.81E-03	0	1.14E-02
115	7.83E-04	1.44E-03	9.10E-03	1.59E-06	1.13E-02
115	9.55E-04	1.81E-03	1.25E-02	2.25E-06	1.53E-02

Note: 1ME5 had no response for the above energies.

Table 3-44. Measured 1MEi and Total Area(0 degrees) for Electrons at GSFC

Electron Energy (keV)	A(0°) (cm2)				
	1ME1	1ME2	1ME3	1ME4	Total
24	1.59E-04	0	0	0	1.59E-04
29.5	5.47E-03	0	0	0	5.47E-03
34.5	9.34E-03	0	0	0	9.34E-03
40	3.68E-02	1.91E-05	0	0	3.68E-02
45	2.14E-02	2.99E-04	0	0	2.17E-02
50	3.02E-02	1.02E-02	0	0	4.04E-02
50	2.85E-02	9.57E-03	0	0	3.80E-02
55	1.70E-02	5.28E-02	1.09E-05	0	6.98E-02
60	8.55E-03	6.00E-02	0.00E+00	0	6.86E-02
75	7.39E-03	9.54E-02	3.16E-05	0	1.03E-01
90	6.24E-03	7.19E-02	4.52E-05	0	7.82E-02
100	8.44E-03	4.43E-02	5.76E-02	0	1.10E-01
115	6.23E-03	1.14E-02	8.81E-02	2.78E-05	1.06E-01
115	8.99E-03	1.64E-02	1.32E-01	2.34E-05	1.57E-01

Note: 1ME5 had no response for these energies

Table 3-45. Measured 1MEi and Total Geometric Factors for Electrons at MIT

Electron Energy (keV)	Gf(E) (cm2-sr)					
	1ME1	1ME2	1ME3	1ME4	1ME5	Total
114	1.10E-02	1.76E-02	6.97E-03	4.87E-04	1.00E-07	3.60E-02
168	2.54E-03	4.68E-03	1.01E-02	1.55E-03	6.94E-07	1.89E-02
261	5.81E-04	1.34E-03	4.62E-03	1.29E-02	2.99E-07	1.94E-02
341	4.58E-04	1.55E-03	3.18E-03	1.86E-02	1.08E-03	2.49E-02
398	3.41E-04	1.52E-03	3.15E-03	8.81E-03	1.06E-02	2.44E-02
520	2.73E-04	4.36E-04	1.44E-03	2.70E-03	1.29E-02	1.78E-02
639	3.39E-04	3.05E-04	1.20E-03	3.07E-03	8.03E-03	1.30E-02
750	1.39E-04	5.12E-04	9.11E-04	4.43E-03	5.46E-03	1.15E-02
813	2.56E-04	4.35E-04	9.18E-04	5.15E-03	5.11E-03	1.19E-02
869	1.33E-04	3.69E-04	1.15E-03	6.02E-03	4.87E-03	1.25E-02
932	1.72E-04	3.98E-04	1.13E-03	6.82E-03	5.22E-03	1.37E-02
997	1.14E-04	3.48E-04	7.28E-04	6.16E-03	4.06E-03	1.14E-02
1251	4.55E-04	3.80E-04	1.17E-03	6.21E-03	3.34E-03	1.16E-02
1515	2.28E-04	3.69E-04	1.76E-03	9.41E-03	4.40E-03	1.62E-02
1724	2.51E-04	4.25E-04	1.76E-03	8.21E-03	2.93E-03	1.36E-02

Table 3-46. Measured 1MEi and Total Area(0 degrees) for Electrons at MIT

Electron Energy (keV)	A(0°) (cm2)					
	1ME1	1ME2	1ME3	1ME4	1ME5	Total
114	2.99E-02	3.22E-02	1.48E-02	2.73E-04	1.00E-07	7.72E-02
168	6.68E-03	6.20E-03	1.40E-02	3.67E-03	4.97E-06	3.06E-02
261	2.57E-03	4.25E-03	1.15E-02	2.53E-02	4.96E-06	4.36E-02
341	6.81E-04	1.40E-03	4.83E-03	2.84E-02	3.28E-03	3.86E-02
398	4.33E-04	1.95E-03	4.60E-03	1.48E-02	2.31E-02	4.49E-02
520	5.62E-04	1.74E-03	3.55E-03	7.31E-03	3.84E-02	5.16E-02
639	8.56E-04	1.20E-03	2.47E-03	9.92E-03	2.53E-02	3.98E-02
750	8.82E-04	1.14E-03	3.14E-03	1.58E-02	1.93E-02	4.02E-02
813	7.96E-04	1.13E-03	2.24E-03	1.97E-02	1.87E-02	4.26E-02
869	1.32E-03	1.32E-03	3.03E-03	2.30E-02	1.99E-02	4.86E-02
932	9.31E-04	1.03E-03	3.11E-03	2.27E-02	1.74E-02	4.52E-02
997	8.78E-04	1.65E-03	3.59E-03	2.97E-02	1.93E-02	5.51E-02
1251	3.11E-04	1.42E-03	5.13E-03	3.33E-02	1.60E-02	5.62E-02
1515	6.32E-04	1.69E-03	8.19E-03	4.87E-02	2.10E-02	8.02E-02
1724	9.15E-04	1.83E-03	7.77E-03	4.29E-02	1.36E-02	6.70E-02

Table 3-47. PM TIROS/NOAA MEPED 0 deg Telescope Electron Calibrations at GSFC

Electron Energy (keV)	Area(0 deg) (cm**2)		Gf (cm**2-sr)	
	0E1	0E2	0E1	0E2
32	0.0103	-	0.00149	-
36	0.0151	-	0.00234	-
41	0.0269	-	0.00442	-
50	0.0369	-	-	-
52	0.0351	-	0.00461	-
82	0.0697	0.00001	0.00932	0.0000015
91	0.0698	0.000129	0.00989	0.0000093
98	0.0791	0.00762	0.0113	0.00105
108	0.0839	0.0348	0.0119	0.00439
118	0.100	0.064	0.0137	0.00815

Table 3-48. PM TIROS/NOAA MEPED 90 deg Telescope Electron Calibrations at GSFC

Electron Energy (keV)	Area(0 deg) (cm**2)		Gf (cm**2-sr)	
	9E1	9E2	9E1	9E2
31	0.0111	-	0.00142	-
40	0.0242	-	0.00305	-
51	0.038	-	0.00514	-
80	0.0704	0.000037	0.00874	0.0000002
89	0.0917	0.000138	0.0123	0.0000097
100	0.1137	0.034	0.0157	0.00386
109	0.1044	0.0764	0.0127	0.00905
119	0.0556	0.0455	0.00704	0.00559

Table 3-49. PM TIROS/NOAA MEPED 0 deg and 90 deg Telescope Electron Calibrations at PL

Electron Energy (keV)	Area(0 deg) (cm**2)		Gf (cm**2-sr)	
	0E1	9E1	0E1	9E1
20	0.000001	0.000003	6.30E-08	1.00E-07
25	0.00019	0.00054	0.000013	0.000052
30	0.00683	0.0177	0.000708	0.00189
35	0.0386	0.0662	0.00419	0.0076
40	0.0598	0.1032	0.00688	0.0127

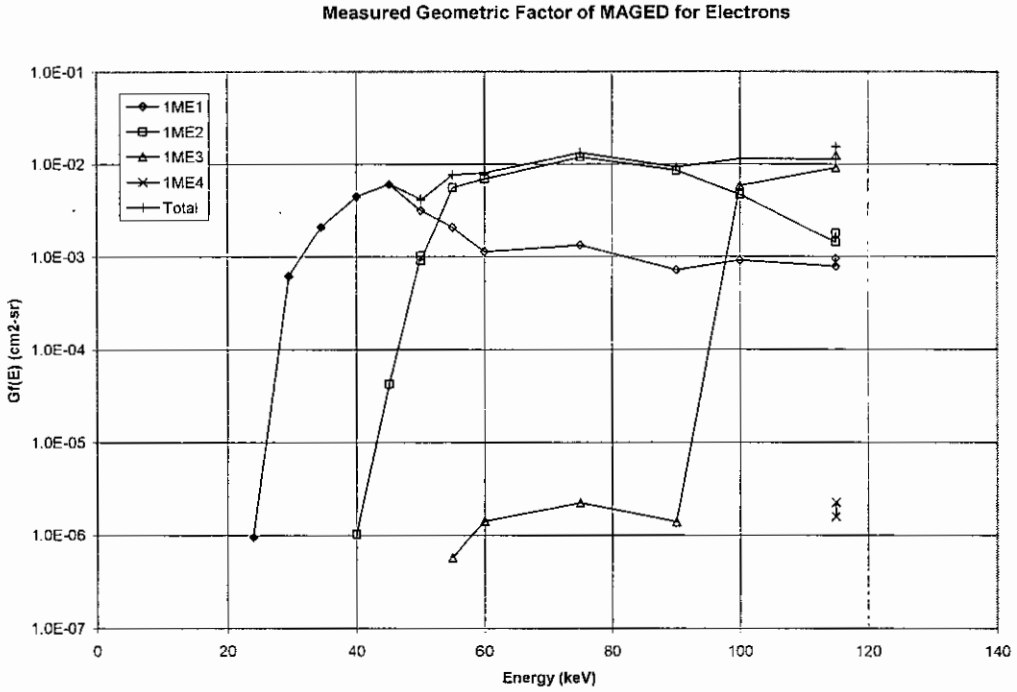

Figure 3-4. MAGED Gf(E) Plots for GSFC Electron Calibration Data

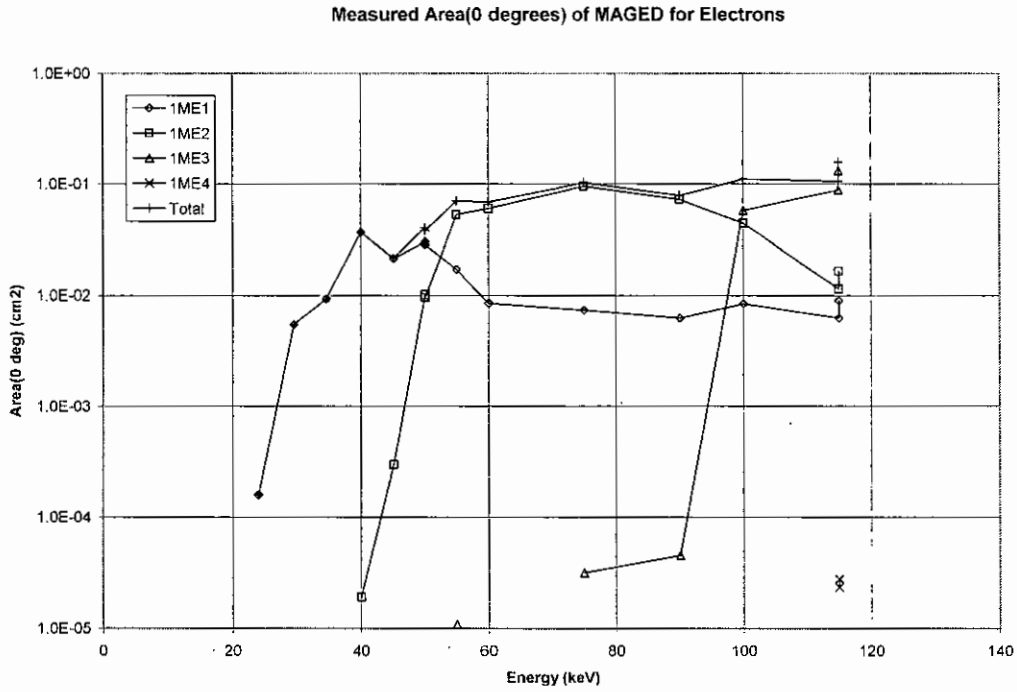

Figure 3-5. MAGED Area(0 deg, E) Plots for GSFC Electron Calibration Data

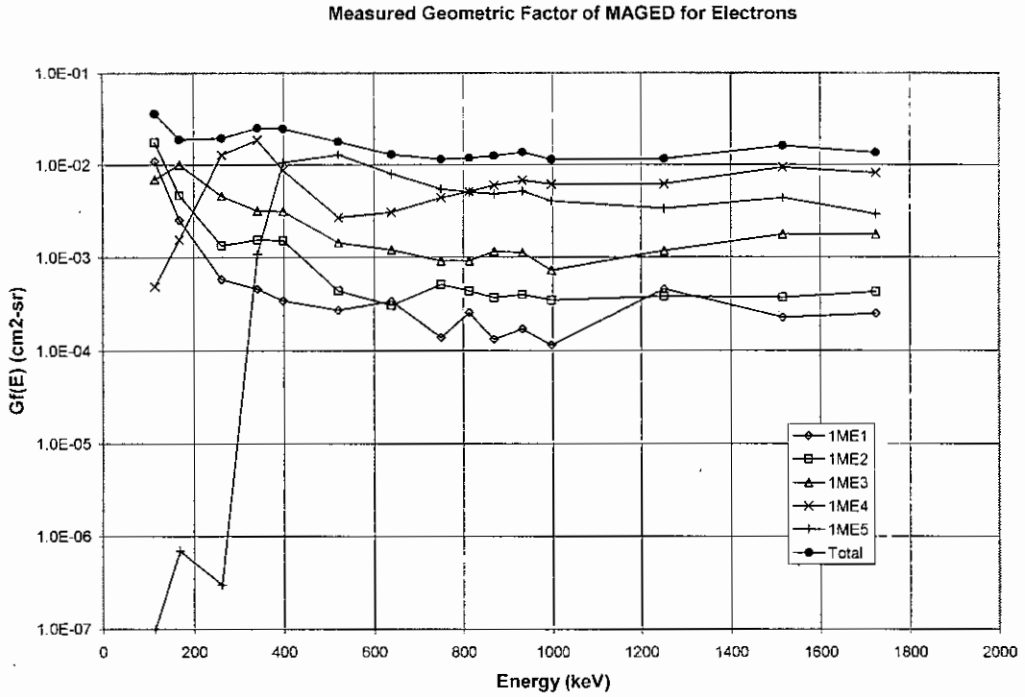

Figure 3-6. MAGED Gf(E) Plots for MIT Electron Calibration Data

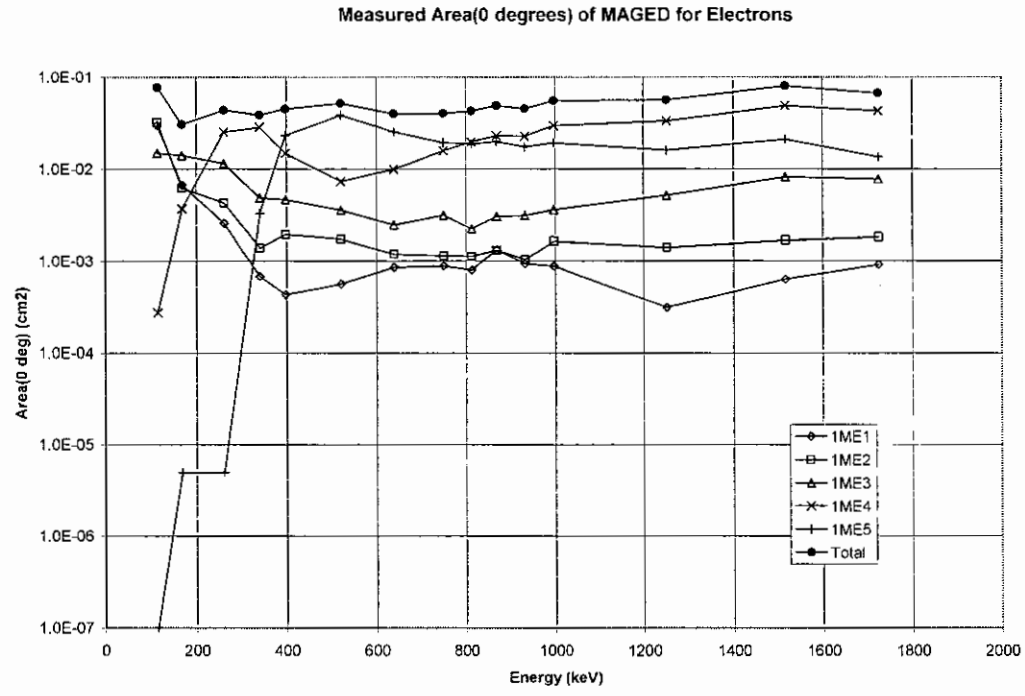

Figure 3-7. MAGED Area(0 deg, E) Plots for MIT Electron Calibration Data

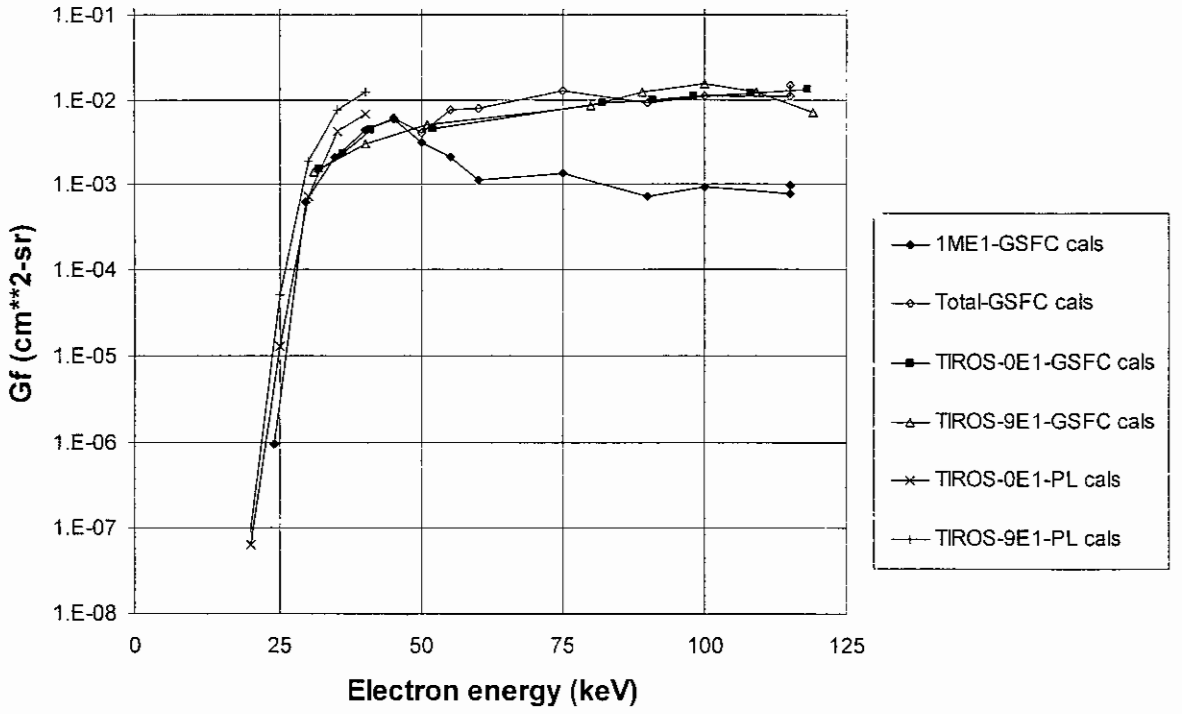

Figure 3-8. MAGED and MEPED Gf(E) Plots for Electron Calibration Data

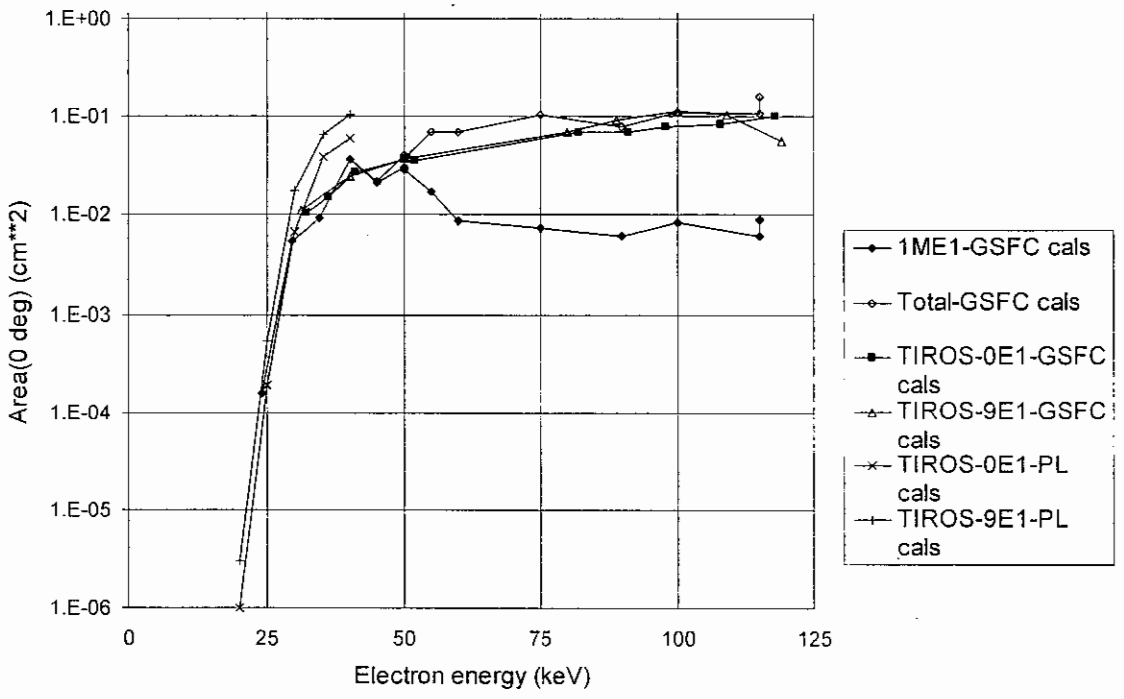

Figure 3-9. MAGED and MEPED Area(0 deg, E) Plots for Electron Calibration Data

3.2.2 Proton Geometric Factors

The measured proton geometric factors, obtained by integrating over the angular measurements given in Tables 3-30 through 3-42, and the A(0) area values, for all 1MEi channels, are summarized in Tables 3-50 and 3-51. The total values in Tables 3-50 and 3-51 are the sum of the five channel values. The results for the GSFC Gf(E) and A(E,0) are shown in Figures 3-10 and 3-11.

The MAGED proton calibrations at the GSFC VdeG have a moderate uncertainty at the highest energies, since it appears that the beam alignment with the calibration chamber may have been slightly off. The highest energy proton calibrations required significant adjustment of the bending magnet and the bending magnet input collimator to achieve measureable counts in the MAGED.

Table 3-50. Measured 1MEi and Total Geometric Factors for Protons at GSFC

Proton Energy (keV)	Gf(E) (cm2-sr)					
	1ME1	1ME2	1ME3	1ME4	1ME5	Total
208	2.92E-03	3.51E-03	1.69E-06	0	0	6.43E-03
228	6.62E-04	4.12E-03	9.57E-05	6.08E-08	0	4.88E-03
246	2.50E-04	5.49E-03	1.24E-03	0	1.20E-06	6.99E-03
292	1.05E-04	3.44E-04	9.03E-03	9.38E-07	0	9.48E-03
394	1.30E-05	4.77E-05	4.11E-05	9.16E-04	1.11E-08	1.02E-03
404	5.59E-05	1.08E-04	2.49E-04	1.63E-02	3.12E-06	1.67E-02
604	2.85E-05	6.86E-05	1.55E-04	2.36E-04	5.08E-03	5.57E-03
608	3.71E-05	7.60E-05	1.51E-04	1.92E-04	3.52E-03	3.98E-03
607	6.78E-06	1.81E-05	6.95E-05	8.58E-05	4.40E-04	6.20E-04
790	4.86E-05	5.19E-05	1.24E-04	1.72E-04	1.79E-04	5.76E-04
795	3.44E-04	1.25E-04	2.05E-04	3.32E-04	4.29E-04	1.44E-03
1052	4.51E-05	8.54E-05	1.58E-04	2.42E-04	4.20E-04	9.50E-04

Table 3-51. Measured 1MEi Area(0 degrees) for Protons at GSFC

Proton Energy (keV)	A(0°) (cm2)					
	1ME1	1ME2	1ME3	1ME4	1ME5	Total
159	3.76E-03	9.39E-05	0	0	0	3.85E-03
181	2.27E-02	3.42E-03	0	0	0	2.61E-02
208	3.37E-02	4.51E-02	1.57E-05	0	0	7.88E-02
228	6.95E-03	4.14E-02	1.07E-03	1.02E-05	0	4.95E-02
246	1.79E-03	4.94E-02	1.35E-02	0	0	6.46E-02
273	1.42E-03	2.48E-02	1.05E-01	5.55E-05	2.77E-06	1.31E-01
292	1.16E-03	2.90E-03	7.48E-02	2.88E-05	0	7.89E-02
394	2.93E-04	3.81E-04	7.61E-04	1.15E-02	1.86E-06	1.29E-02
404	3.45E-04	8.22E-04	2.70E-03	1.16E-01	1.62E-05	1.20E-01
604	1.73E-04	1.32E-03	2.30E-03	3.70E-03	4.04E-02	4.79E-02
608	4.89E-04	6.65E-04	1.19E-03	1.74E-03	2.95E-02	3.35E-02
607	2.48E-04	3.87E-04	6.61E-04	1.18E-03	1.01E-02	1.26E-02
790	4.15E-04	4.15E-04	1.23E-03	2.49E-03	3.32E-03	7.87E-03
795	3.33E-03	7.09E-04	1.61E-03	3.03E-03	4.29E-03	1.30E-02
896	5.18E-04	2.96E-04	4.81E-04	1.36E-03	2.44E-03	5.09E-03
1052	2.34E-04	8.81E-04	1.45E-03	2.74E-03	5.35E-03	1.07E-02

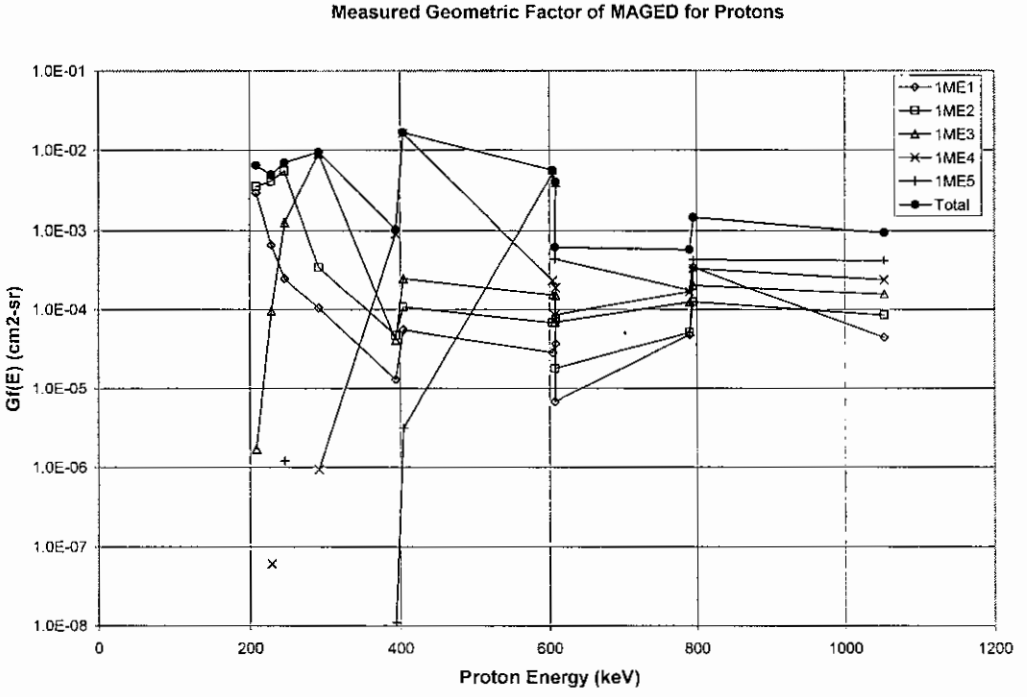

Figure 3-10. MAGED Gf(E) Plots for GSFC Proton Calibration Data

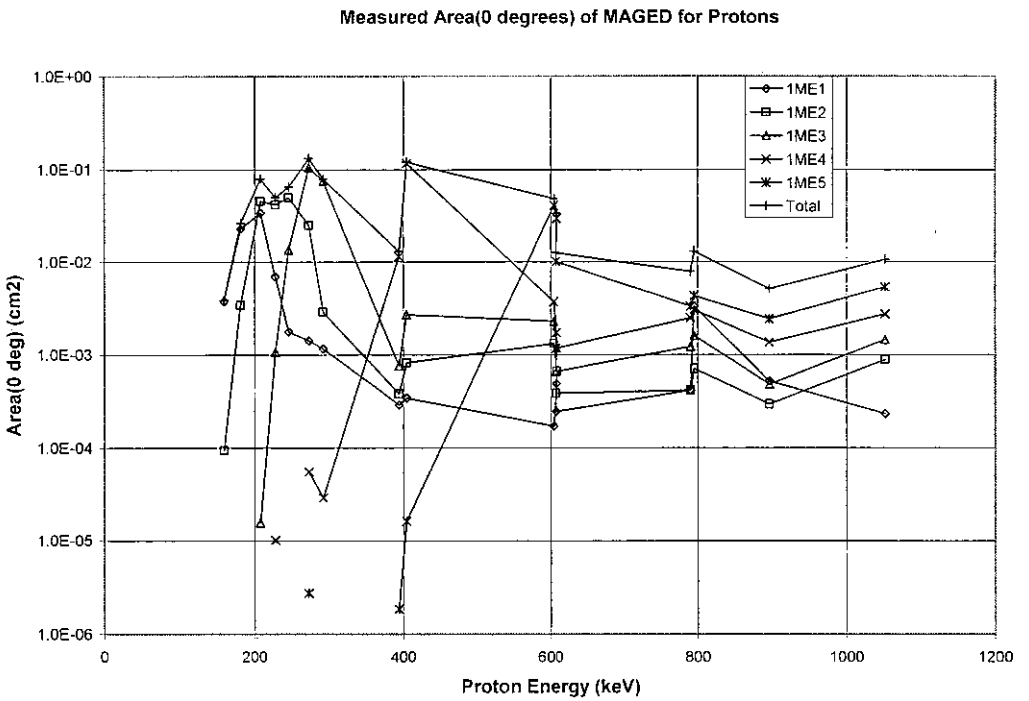

Figure 3-11. MAGED Area(0 deg, E) Plots for GSFC Proton Calibration Data

3.3 Comparison of Measured and Calculated Responses

3.2.1 Calculated Responses

The design of the MAGED telescope is shown in Figure 2-1, and the calculated electron and proton energy losses in the SSD are shown in Figure 3-12. The energy losses are calculated from the stopping powers given in Refs. 4 and 5 for electrons, and in Ref. 6 for protons. The Area(0 degrees) = 0.0856 cm^2, and the total geometric factor is Gf = 0.0100 cm^2-sr. The channel energy breakpoints are listed in Table 3-52.

The calculations assume a nominal Ni foil thickness of 0.68 mg/cm^2 and a SSD thickness of 700 um Si. Proton energy deposits are expected to be reasonably accurate, since there is minimal scattering of protons in the Ni foil and the Si SSD. At very high energies the proton energy loss drops because the dE/dx energy loss decreases and the protons penetrate the SSD. The stopping power (dE/dx) reaches a minimum at about 2000 MeV, so the high energy proton energy loss never goes below the lower threshold for ME4.

Electrons scatter significantly, and for the highest energy electrons (>>1 MeV) there will be a significant fraction depositing the ionization energy loss value, although this will be a broad distribution in energy. Thus the ME3, ME4, and ME5 channels are expected to have a moderate high energy electron response, as shown in the MIT data in Figure 3-6.

The measured electron and proton data are in reasonable agreement with the calculations, with the A(0 degrees) values generally being near 0.0856 cm^2 for full channel (or summed-channel) responses, and the Gf values (generally for the channel-summed values) are near 0.010 cm^2-sr. The electron calibrations are discussed in more detail in Section 3.3.2, with best-fit Gf(E) functions being provided for data analysis. The proton calibrations are discussed in more detail in Section 3.3.3, with best-fit Gf(E) functions being provided for use in correction of the electron flux data using the MAGPD measurements.

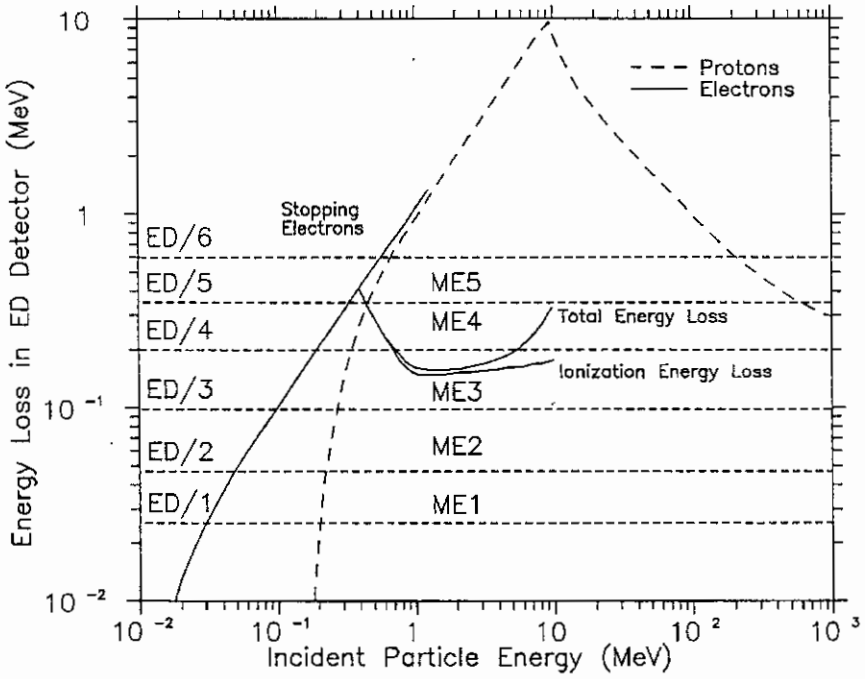

Figure 3-12. MAGED Telescope Energy Loss Curves

Table 3-52. Calculated Electron and Proton MAGED Channel Energies

Threshold Values and Particle Energies					Channel Logic	
Threshold No.	Threshold Value (keV)	Electron Energy (keV)	Low Proton Energy (keV)	High Proton Energy (MeV)	MAGED Channel	Threshold Range
Level 1	25.6	30.	209.	-	ME1	1 to 2
Level 2	47.0	50.	230.	-	ME2	2 to 3
Level 3	98.	100.	274.	-	ME3	3 to 4
Level 4	199.	200.	358.	-	ME4	4 to 5
Level 5	349.	350.	487.	564.	ME5	5 to 6
Level 6	599.	600.	712.	197.		

3.3.2 Electron Responses

The MAGED electron channel Gf(E) measurements are given in Tables 3-43 and 3-45, and plotted in Figures 3-4 and 3-6, with additional comparisons in Figure 3-8. A better estimate of the energies where the response switches from one channel to another can be made by viewing a plot of the fractional A(0 deg), where each channel has its measured area divided by the total channel summed area. Figure 3-13 shows a plot of all of the GSFC and MIT relative measured A(0 deg) data, while Figure 3-14 shows the low energy GSFC data in a more readable scale. Using these plots, the electron energies for channel switches are listed in Table 3-53, along with the calculated values from Table 3-52.

The measured electron transition energies agree well with the calculated values, with the following comments:

1. The lowest energy threshold is closer to 35 keV, mostly because of the effects of electron scattering in the Ni foil. This raises the lowest energy threshold slightly, although the effective channel thrshold is still close to 30 keV.

2. The three highest energy thresholds are all slightly larger than the calculated values, mostly because of the effects of the electron energy loss peak shifting from the total energy loss peak to the dE/dx peak (see Figure 3-12). This shift gives the highest energy channels a long high energy electron detection tail. Note that 1ME4 in Figure 3-13 shows the beginning of a high energy detection band at about 800 keV, from the electron dE/dx peak.

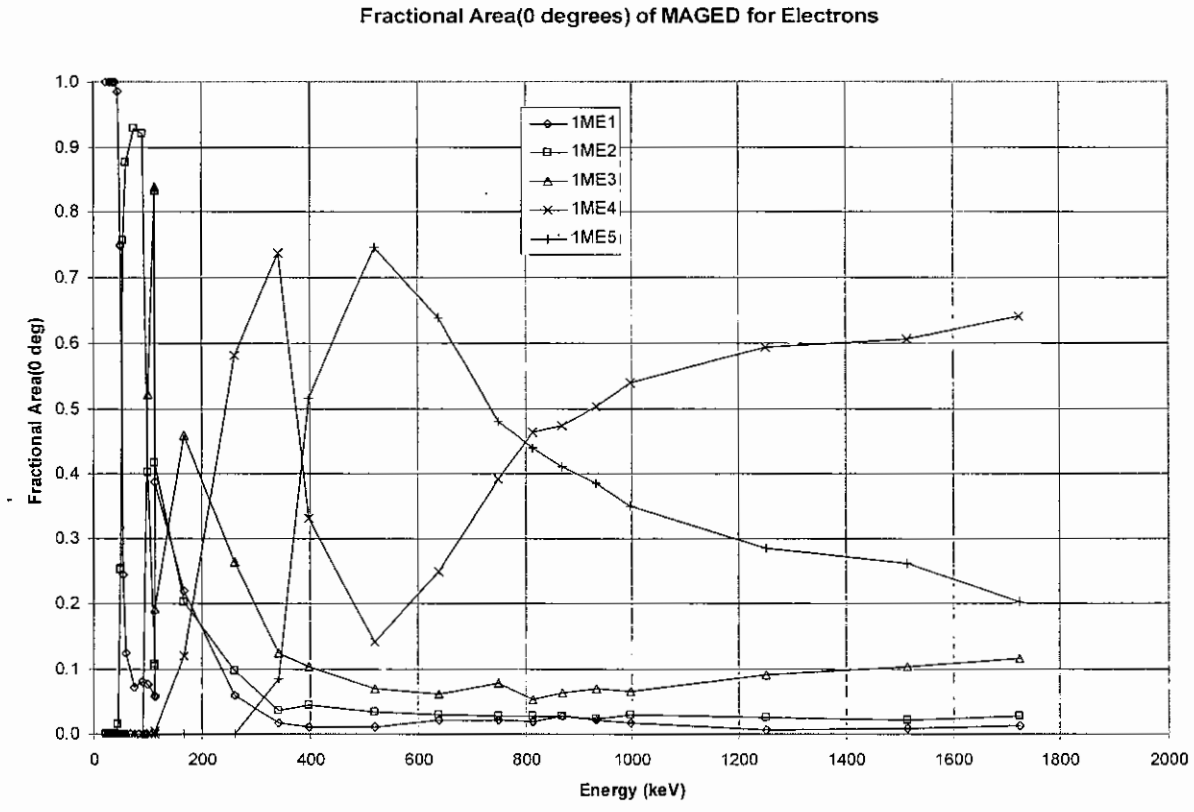

Figure 3-13. Measured Relative 1MEi A(0 deg) Values as a Function of Electron Energy

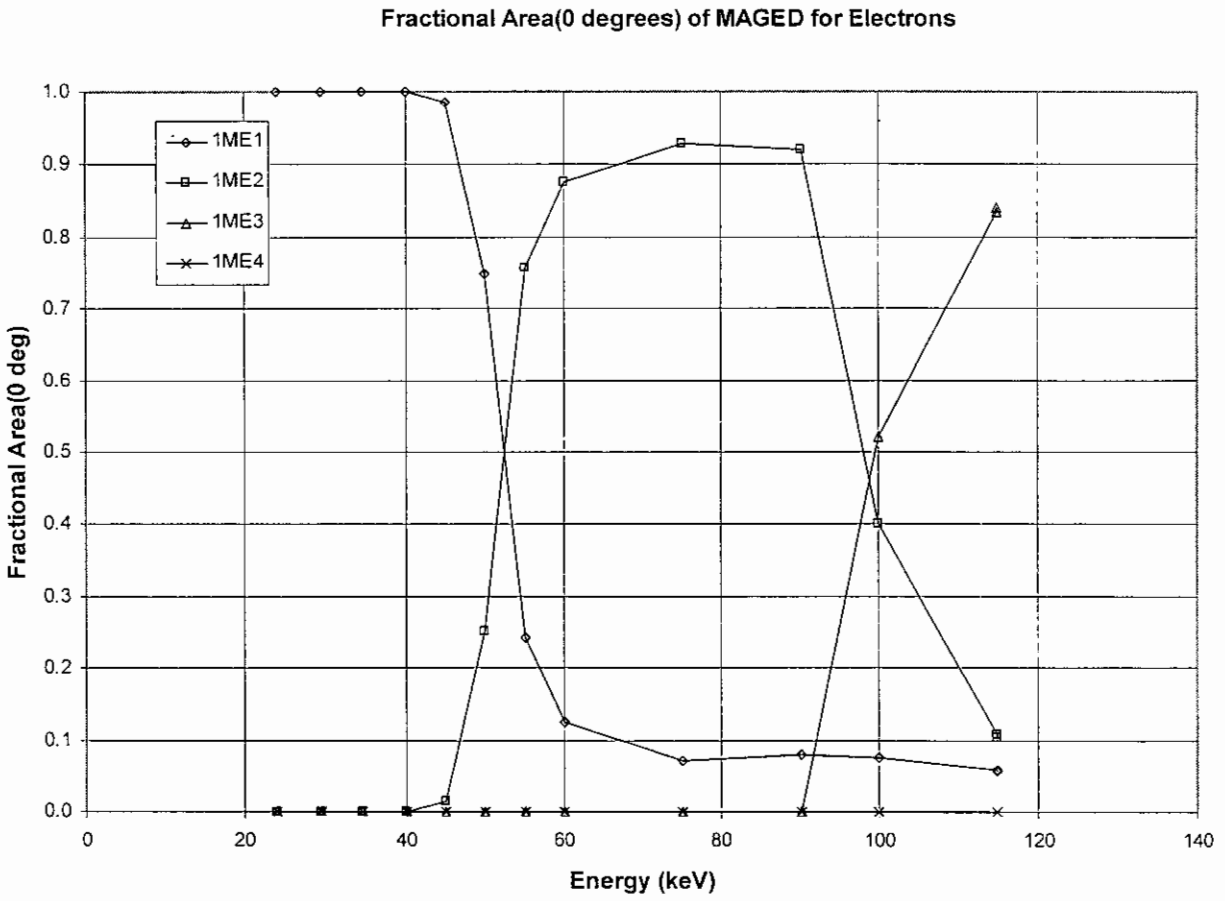

Figure 3-14. Measured Relative 1MEi A(0 deg) Values as a Function of Electron Energy for GSFC Data

Table 3-53. Measured MAGED Electron Channel Transition Energies

Threshold Level	Channel Transition	Transition Energies (keV)	
		Calculated	Measured
Level 1	ME1 / On	30	35
Level 2	ME1 / ME2	50	52.5
Level 3	ME2 / ME3	100	99
Level 4	ME3 / ME4	200	220
Level 5	ME4 / ME5	350	380
Level 6	ME5 / Off	600	750

The MAGED electron channel measured responses are close to the calculated responses, with a high energy tail from the dE/dx energy loss peak. The recommended effective electron energy-geometric factors for the MAGED electron channels are listed in Table 3-54, and shown for each individual channel, along with the measured data, in Figures 3-15 to 3-19.

Table 3-54. Recommended MAGED Electron Channel Gf(E) Values for Electrons

ME1 Gf(E)		ME2 Gf(E)		ME3 Gf(E)		ME4 Gf(E)		ME5 Gf(E)	
Energy (keV)	Gf(E) (cm^2-sr)	Energy (keV)	Gf(E) (cm^2-sr)	Energy (keV)	Gf(E) (cm^2-sr)	Energy (keV)	Gf(E) (cm^2-sr)	Energy (keV)	Gf(E) (cm^2-sr)
25	3.0E-5	45	3.0E-5	95	1.0E-4	190	1.0E-3	350	1.0E-3
35	1.0E-2	55	1.0E-2	105	1.0E-2	220	1.0E-2	400	1.0E-2
45	1.0E-2	95	1.0E-2	200	1.0E-2	350	1.0E-2	600	1.0E-2
60	1.0E-3	110	1.0E-3	500	1.0E-3	500	3.0E-3	1000	4.0E-3
200	1.0E-3	250	1.0E-3	2000	1.0E-3	800	6.0E-3	2000	3.0E-3
500	2.0E-4	500	4.0E-4			2000	1.0E-2		
2000	2.0E-4	2000	4.0E-4						

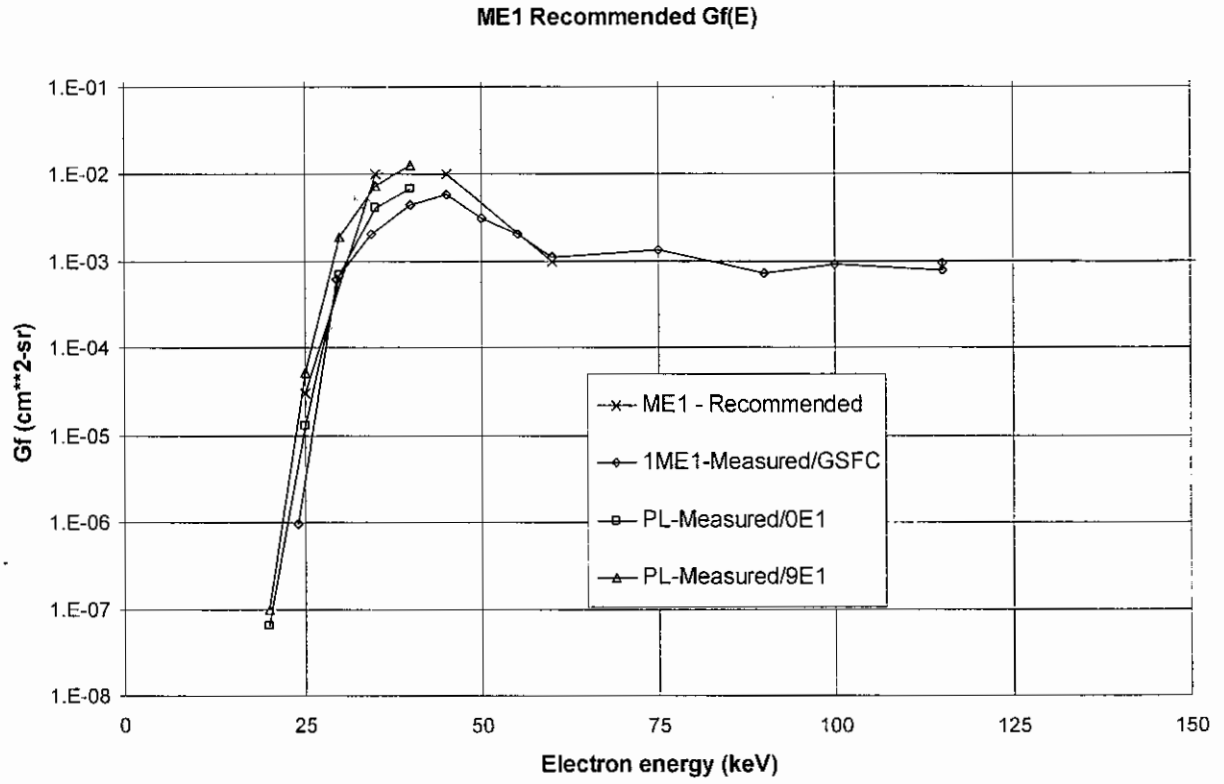

Figure 3-15. Recommended and Measured ME1 Gf(E) Values as a Function of Electron Energy

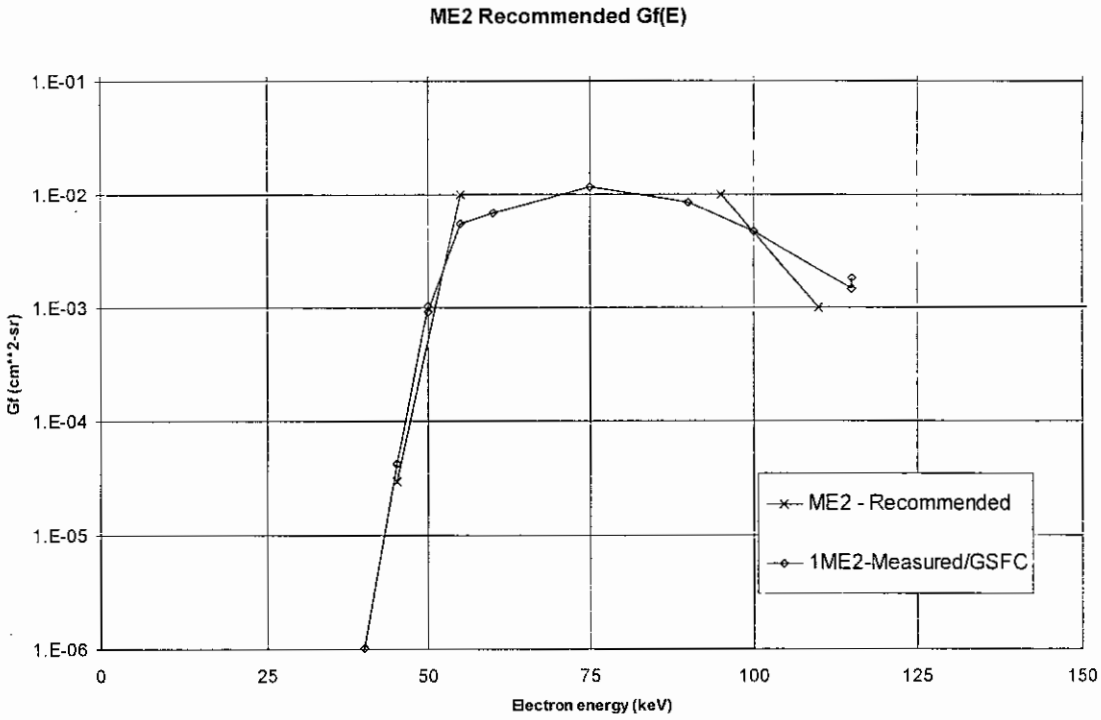

Figure 3-16. Recommended and Measured ME2 Gf(E) Values as a Function of Electron Energy

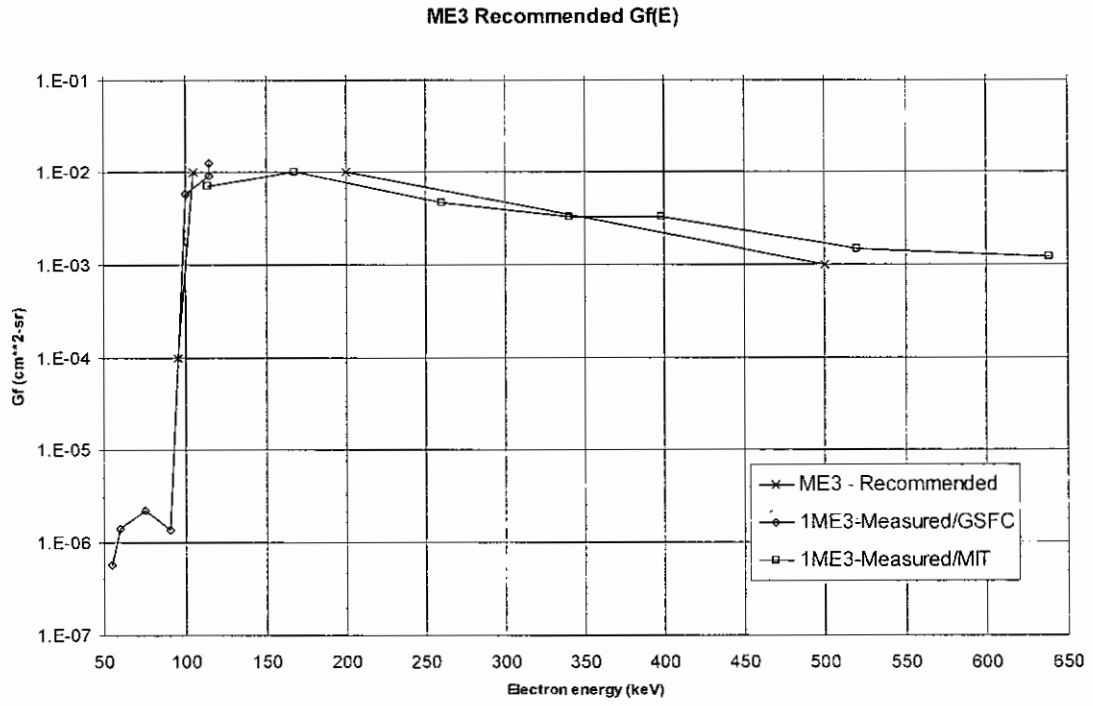

Figure 3-17. Recommended and Measured ME3 Gf(E) Values as a Function of Electron Energy

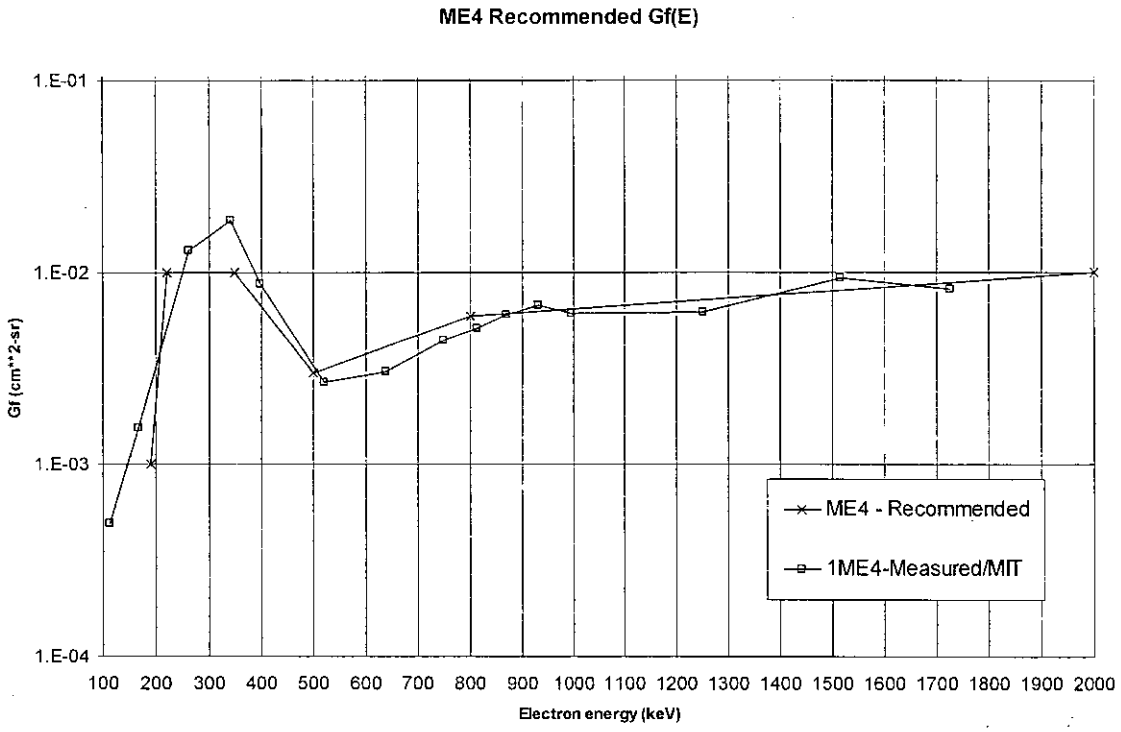

Figure 3-18. Recommended and Measured ME4 Gf(E) Values as a Function of Electron Energy

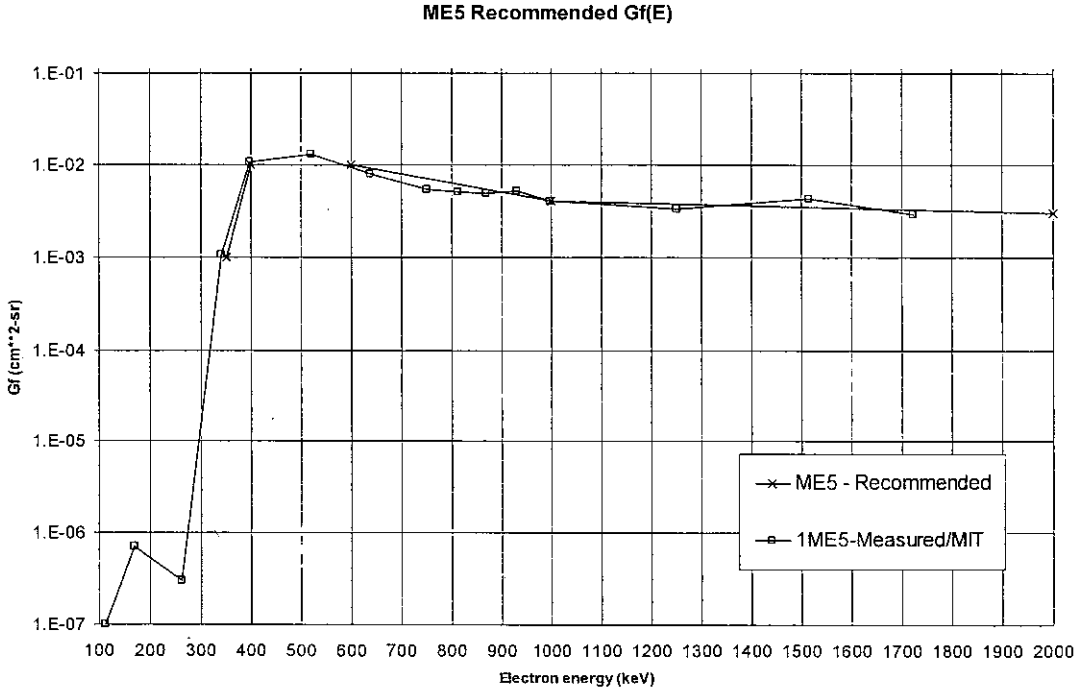

Figure 3-19. Recommended and Measured ME5 Gf(E) Values as a Function of Electron Energy

The ME1 channel has a recommended response very close to the calculated response. The rise and fall edges have about a 10 KeV width, mostly from the FWHM noise of the SSD, although the rising edge has some width from electron scattering in the Ni foil. There is a slight high energy tail up to about 200 keV, which falls off even more up to 2000 keV. The high energy tail is mainly from electrons which scatter out of the SSD before depositing all of their energy.

The ME2 channel has a recommended response very close to the calculated response. The rise and fall edges have about a 10 KeV width, mostly from the FWHM noise of the SSD. There is a slight high energy tail up to about 250 keV, which falls off even more up to 2000 keV. The high energy tail is mainly from electrons which scatter out of the SSD before depositing all of their energy.

The ME3 channel has a recommended response close to the calculated response, with a slight broadening of the high energy edge. The rise edge has about a 10 KeV width, mostly from the FWHM noise of the SSD. The fall edge is broadened because the electron energy is near the range-thickness of the SSD, and the dE/dx energy loss peak is beginning to appear. The high energy tail is about 10% of the peak Gf of 0.010 cm^2–sr, and extends up to 2000 keV. The high energy tail is mainly from the low energy side of the broad dE/dx energy loss peak for electrons in the SSD.

The ME4 channel has a recommended response close to the calculated response, with a moderate broadening of the high energy edge. The rise edge has about a 20 KeV width, partly from the FWHM noise of the SSD, but mostly from the straggling in the electron energy loss distribution in the SSD. The fall edge is broadened and increased in energy because the electron energy is past the range-thickness of the SSD, and the dE/dx energy loss peak is becoming dominant. The high energy tail is about 30% of the peak Gf of 0.010 cm^2–sr at its minimum near 500 keV, and then increases up to 2000 keV. The high energy tail is primarily from the dE/dx energy loss deposit by electrons in the SSD (see Figure 3-12).

The ME5 channel has a recommended response slightly higher in energy than the calculated response. The rise edge is shifted to nigher energies because the electron dE/dx energy loss peak is shifting electron detection into the ME4 channel. The fall edge is approximately at the correct energy of 600 keV, but has an exteneded high energy tail because the dE/dx energy loss peak is dominant. The high energy tail drops to about 30% of the peak Gf of 0.010 cm^2–sr at 2000 keV. Note that for electron energies >800 keV the ME4 channel is more efficient at detection than the ME5 channel.

The calibrated electron Gf(E) responses can be used to calculate electron spectra from the measured channel count rates. This involves integrating assumed spectral shapes over the Gf(E) curves, and determining the spectral parameters from the best fit to the measured data. The recommended Gf(E) values should be used, and are estimated to be accurate to +/-25%.

3.3.3 Proton Responses

The MAGED electron channel Gf(E) measurements for protons are given in Table 3-50, and plotted in Figure 3-10. A better estimate of the energies where the response switches from one channel to another can be made by viewing a plot of the fractional A(0 deg), where each channel has its measured area divided by the total channel summed area. Figure 3-11 shows a plot of the GSFC measured A(0 deg) data, while Figure 3-20 shows the fractional A(0 deg) responses. Using these plots, the proton energies for channel switches are listed in Table 3-55, along with the calculated values from Table 3-52.

The measured proton transition energies agree well with the calculated values, with the following comments:

1. The four lowest energy thresholds are lower than the calculated values by 15-30 keV. This may be caused by the Ni foil being slightly thinner than the nominal 0.68 mg/cm^2; a 10% thinner foil can explain the difference, and is within the uncertainties of the alpha particle thickness measurements made on the foils.

2. The two highest energy thresholds are approximately correct, but the proton energy data are too sparse to determine the actual transition energies more accurately.

3. The measured geometric factors are close to the calculated value of 0.010 cm^2-sr, allowing for the problems with proton beam alignment at GSFC.

The recommended effective low energy proton energy-geometric factors for the MAGED electron channels are listed in Table 3-56, and for the high energy proton range in Table 3-57. The low energy range is given for all five channels, while the high energy range applies only to the two highest energy channels. The recommended values for proton energies are the calculated values, since this is expected to be applicable to all MAGED units. The slight shift in energies because of a +/-10% Ni foil thickness variation should not affect the proton contamination calculations significantly. The estimated accuracy of the recommended proton responses is about +/-25%.

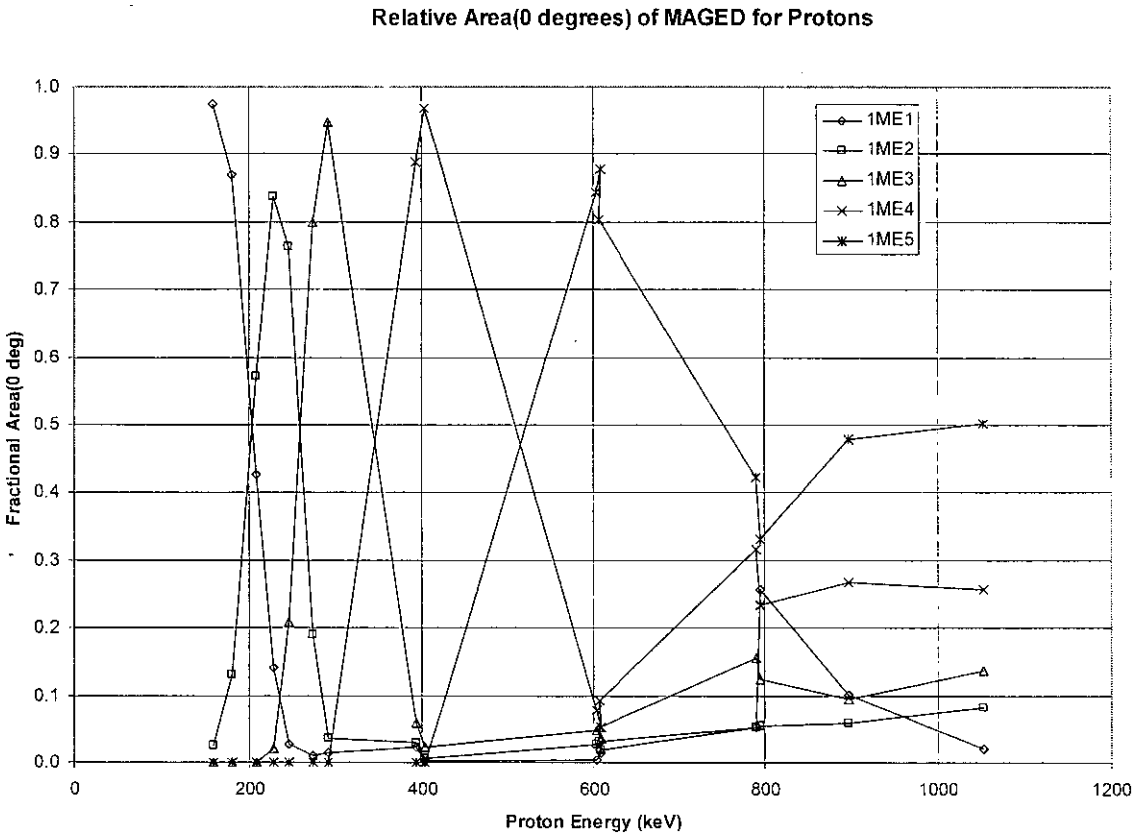

Figure 3-20. Measured Relative 1MEi A(0 deg) Values as a Function of Proton Energy

Table 3-55. Measured MAGED Proton Channel Transition Energies

Threshold Level	Channel Transition	Transition Energies (keV)	
		Calculated	Measured
Level 1	ME1 / On	209	180
Level 2	ME1 / ME2	230	200
Level 3	ME2 / ME3	274	260
Level 4	ME3 / ME4	358	340
Level 5	ME4 / ME5	487	(500)
Level 6	ME5 / Off	712	(700)

Table 3-56. Recommended MAGED Electron Channel Gf(E) Values for Low Energy Protons

ME1 Gf(E)		ME2 Gf(E)		ME3 Gf(E)		ME4 Gf(E)		ME5 Gf(E)	
Energy (keV)	Gf(E) (cm^2-sr)	Energy (keV)	Gf(E) (cm^2-sr)	Energy (keV)	Gf(E) (cm^2-sr)	Energy (keV)	Gf(E) (cm^2-sr)	Energy (keV)	Gf(E) (cm^2-sr)
205	0.0	225	0.0	270	0.0	355	0.0	480	0.0
210	0.010	235	0.010	280	0.010	365	0.010	490	0.010
225	0.010	270	0.010	355	0.010	480	0.010	705	0.010
235	0.0	280	0.0	365	0.0	490	0.0	715	0.0

Table 3-57. Recommended MAGED Electron Channel Gf(E) Values for High Energy Protons

ME1 Gf(E)		ME2 Gf(E)		ME3 Gf(E)		ME4 Gf(E)		ME5 Gf(E)	
Energy (MeV)	Gf(E) (cm^2-sr)	Energy (MeV)	Gf(E) (cm^2-sr)	Energy (MeV)	Gf(E) (cm^2-sr)	Energy (MeV)	Gf(E) (cm^2-sr)	Energy (MeV)	Gf(E) (cm^2-sr)
-	-	-	-	-	-	564.	0.0	197.	0.0
						564.	0.010	197.	0.010
						(infinite)	0.010	564.	0.010
								564.	0.0

4.0 SUMMARY AND CONCLUSIONS

The MAGED 1MEi electron channel responses have been calibrated with electron and proton beams at accelerators at GSFC and MIT. The results are in reasonable agreement with previous calibrations of these channels. The calibrated geometric factors can be used to reduce in-orbit count rate data to electron fluxes. The energy and angular responses are in reasonable agreement with the expected theoretical responses.